CHALMERS
UNIVERSITY OF TECHNOLOGY

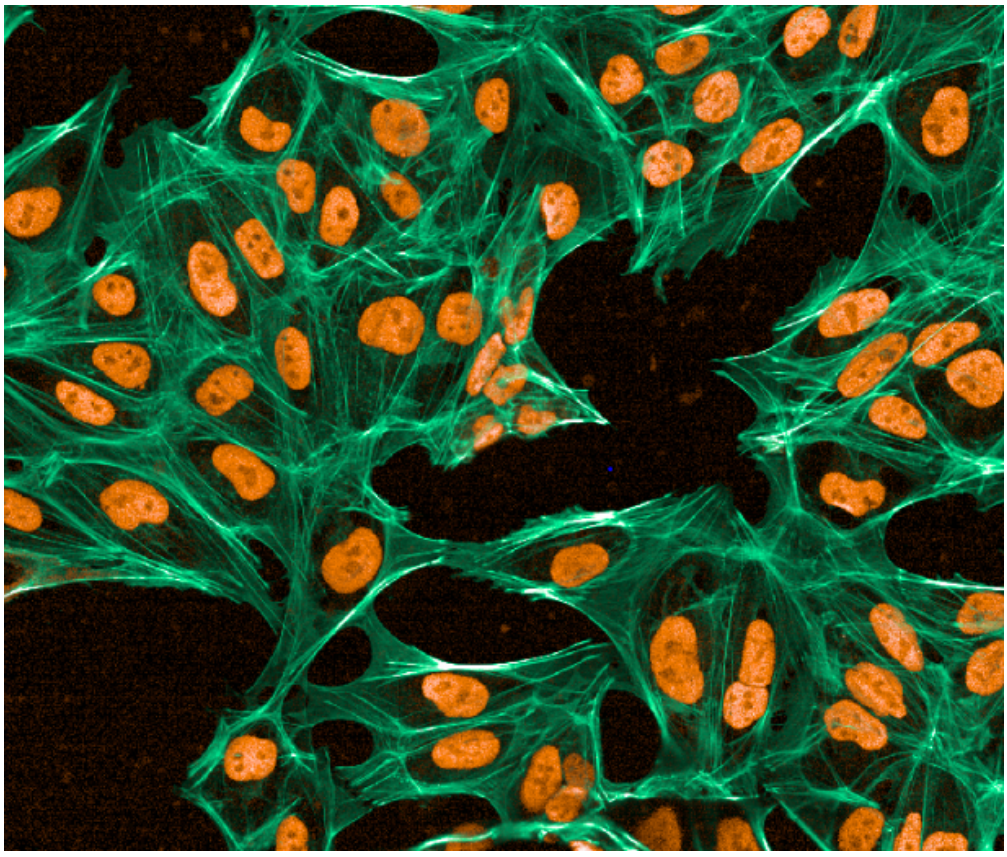

Inducible forward programming of human induced pluripotent stem cells to skeletal myocytes

Master's thesis in Biotechnology

EMIL LÖFGREN

DEPARTMENT OF LIFE SCIENCES

CHALMERS UNIVERSITY OF TECHNOLOGY
Gothenburg, Sweden 2024
www.chalmers.se

Master's thesis 2024

Inducible forward programming of human induced pluripotent stem cells to skeletal myocytes

EMIL LÖFGREN

CHALMERS
UNIVERSITY OF TECHNOLOGY

AstraZeneca,
Genome Engineering Technologies
Department of Life Sciences
Chalmers University of Technology
Gothenburg, Sweden 2024

Master's thesis
Inducible forward programming of human induced pluripotent stem cells to skeletal myocytes
EMIL LÖFGREN

Supervisor: Antje Rottner, Senior Scientist in Genome Engineering Technologies at AstraZeneca.
Examiner: Yvonne Nygård Associate Professor at Department of Life Sciences, Chalmers University of Technologies

Master's Thesis 2024
Department of Life Sciences
Chalmers University of Technology
SE-412 96 Gothenburg
Telephone +46 31 772 1000

Cover: hiPSCs stained for OCT4 (orange) and Actin (green).

Typeset in LaTeX
Printed by Chalmers Reproservice
Gothenburg, Sweden 2024

Inducible forward programming of human induced pluripotent stem cells to skeletal myocytes
EMIL LÖFGREN
Department of Life Sciences
Chalmers University of Technology

Abstract

Differentiation of human induced pluripotent stem cells into a desired phenotype is challenging. Previous attempts of hiPSC differentiation into skeletal myocytes using an in-house protocol has resulted in heterogeneous populations of cells. Resolving the heterogeneity of Skeletal myocyte differentiation is key for acquiring tissues and cell types suited for exploring novel therapies and mechanisms within muscle related diseases. Thus the main objective of this thesis was to investigate if alterations in gene expression could resolve the heterogeneity of the differentiation process of Skeletal Myocytes. In this thesis, differentiation of hiPSCs into skeletal myocytes was explored through modulation of the transcription factors MYOD1 and OCT4 using the genome editing enrichment method "Xential".
The addition of the HBB IVS2 intron sequence led to a 2-fold increase in *MYOD1* expression, furthermore adjustments to the seeding density led to an additional 2-fold increase of *MYOD1*. Knockdown efficiency of shRNA targeting *POU5F1* is correlated with the seeding density. The downstream marker of myogenesis *DES* had a 15-fold increase when seeding density was adjusted. This correlation between differentiation efficiency and seeding density highlights the interplay between environmental pressures and gene expression. The HBB IVS2 intron sequence led to higher homogeneity in the cultures, this provides insights into future strategies to mitigate heterogeneity in hiPSC differentiation.

Keywords: Skeletal Myocytes, hiPSC, iPSC, MYOD1, OCT4, Seeding Density, Xential, Diphtheria Toxin, differentiation, HBB ISV2.

Acknowledgements

This thesis has been a long journey for me with a lot of trials and tribulations. I would like to extend my sincere gratitude to several individuals who have made it possible for me to complete the thesis.
First, I am deeply grateful to my supervisor Dr. Antje Rottner. Without her, there would be no project at all. Her diligence, patience and constructive feedback made writing the thesis seem less daunting and I could not ask for a better person to learn from.
I would also like to extended my thanks to my line manager Dr. Grzegorz Sienski who encouraged me to pursue anything and everything I was curious about. He also kept me properly nervous when I presented updates on the project.
By extension I am indebted to the genome engineering department for being generous enough to allow a master thesis student to pursue a project with their resources and expertise.
I extended my appreciation to Yvonne Nygård for her evaluation of the project as well as the feedback she has provided throughout the project. Without her initial feedback the thesis would look quite different.
I'd like to extend my thanks to Mauritz Khööler who not only helped proof read the thesis but also debugged and assisted in formatting the entire thesis. He has once again proven to be a steadfast and reliable friend.
Lastly, I want to thank all of my friends, colleagues and fellow students who supported me throughout this journey. Thank you all for your contributions and support.

List of Acronyms

Below is the list of acronyms that have been used throughout this thesis listed in alphabetical order:

CRISPR	Clustered Regularly Interspaced Short Palindromic Repeat
Ctrl	Control
DES	Desmin
Dox	Doxycyclin
DT	Diphtheria Toxin
GOI	Gene of Interest
hiPSC	Human Induced Pluripotent Stem Cell
Indel	Insertion or deletion
iPSC	Induced Pluripotent Stem Cell
mNG	Monomeric NeonGreen
MYOD1	Myogenic Differentiation 1
OCT4	Octamer-binding transcription factor 4
PAM	Protospacer adjacent motif
PCR	Polymerase Chain Reaction
sh	Short hairpin
sgRNA	Single-guide RNA
RT-qPCR	Reverse transcriptase quantitative polymerase chain reaction
WT	Wild-type

Contents

List of Figures

List of Tables

1

Introduction

1.1 Background

Generating cell types directly from human induced pluripotent stem cells (hiPSC) can be of great benefit for fields such as drug discovery, drug testing and *in vitro* disease modelling [1, 2]. There is hope that through the study of particular cell types, it will be possible to cure some genetic diseases such as muscle dystrophies [1, 3]. However, *in vitro* derivation and differentiation of human stem cells is a challenging task and remains inefficient. Of particular interest to this study are skeletal myocytes because there is a range of disease and targets relevant for drug development which are connected to muscle tissue.

Currently there are four main platforms to acquire skeletal myocytes, commercial skeletal myocytes, human primary muscle tissue, primary muscle tissue from rodents and rodent cell lines [4]. Commercial skeletal myocytes are expensive, offer limited options for genome editing and customization, do not contain potential mutations of interest and require from days, to several weeks, to months to acquire functional skeletal myocytes.

Primary muscle tissue remains an option, however it is an invasive method to retrieve the tissue from patients. Secondly, it offers limited opportunities for genome editing and customization. Lastly it introduces donor variability as a factor to consider, if cells are retrieved from healthy donors the mutation or variation of interest needs to be introduced [5].

Rodent cell lines can be considered, they are generally more cost-effective than hiPSCs and provide a good platform to investigate several phenomenona, however they have been shown to respond differently to treatments compared to human cell lines, such as response to the weak androgen Dehydroepiandrosterone (DHEA). Furthermore, their protein expression differs as rodents have a higher proportion of fast twitch fibers, express some proteins that are not present in humans such as myosin heavy chain 2b. Simply put, their mechanisms are different as a result of different demands on the cells compared human skeletal myocytes [6, 7, 8]. With these options in mind, developing an in-house protocol to acquire skeletal myocytes from hiPSCs is valuable for future projects [3]. With the AZ-proprietary genome editing enrichment method "Xential" it has internally been shown that it is possible to differentiate hiPSCs to skeletal myocytes. However, the efficiency is low and a more robust protocol is needed, as the method produces highly heterogeneous cell populations. If functional studies of disease associated variants are to be conducted, a better protocol needs to be established [9].

1.1.1 Human Induced Pluripotent Stem Cells

Induced pluripotent stem cells (iPSCs) are created through treating adult somatic cells, often skin or blood cells, with specific transcription factors to make them pluripotent. To generate human iPSCs (hiPSCs) Octamer binding transcription factor 4 (OCT4) and sex-determining region Y-box 2 (SOX2), were shown to be two of the essential transcription factors required to program human somatic cells into stem cells [10, 11]. hiPSCs can be identified by their morphology, expression of pluripotency markers and DNA methylation profile [12]. The morphology of hiPSC in culture is distinct borders and well-defined edges. As they are fragile and prone to apoptosis, cell to cell contact is preferred though how much contact varies depending on the culturing system [13]. hiPSCs share many characteristics with human embryonic stem cells and have been shown to be able to differentiate into various cell types such as cardiomyocytes and endothelial cells [14, 15]. Through years of trial and error there are now established methods to keep hiPSCs in culture while maintaining pluripotency.

1.1.2 Skeletal Myocytes

Skeletal myocytes or skeletal muscle cells are found in several tissues in the body. They help the body move and respond to stimuli through contraction and relaxation. Most skeletal myocytes, unlike cardio myocytes, are responsive to neural inputs. Skeletal myocytes constitutes approximately 40% of total human body weight and contains more than half of all the body's proteins [16]. Although each and every skeletal myocyte has their own neural connection, they tend to form into bundles, aligning themselves longitudinally and are best described as fibers [17]. During formation of skeletal muscle fibers, several myocytes fuse to contain multiple nuclei within one membrane [18]. There is a range of proteins that are expressed in skeletal myocytes, examples of these are Myogenic differentiation 1 (MYOD1), Desmin (DES) and Myogenin Heavy Chain 1 (MYH1) [19].

1.1.3 Genes of Interest

OCT4 is encoded by *POU5F1*, and is critical in sustaining pluripotency of cells. It is commonly used to identify totipotent embryonic stem cells [20]. OCT4 has been frequently shown to be able to induce somatic cells into stem cells with the help of other transcription factors [21, 11]. The down regulation of *POU5F1* has been shown to support cells in their ability to lose their pluripotency and commit to a phenotype [3]. Thus suppressing the expression of *POU5F1* will suppress the hiPSCs ability to stay pluripotent, this is crucial to urge the cells to commit to a cell type [3, 20].
Myogenic differentiation 1 encoded by *MYOD1* is a master transcriptional regulator of myogenesis, Myogenesis is the muscle development and formation process which can result in multinucleated myofibers capable of contraction [22, 23]. As early as 2012 attempts at direct programming hiPSCs to skeletal myocytes were published where a dox-inducible lentivirus system was used [24]. The protocols have since then been improved on and overtime MYOD1 has become one of the transcription

factors frequently used to induce cells into skeletal myocytes [3, 25]. In some cases it was discovered overexpression of *MYOD1* is sufficient to create skeletal myocytes from hiPSCs [26, 27]. However, overexpression of *MYOD1* alone can also result in cell death [28]. Furthermore, overexpression of *MYOD1* in combination with retonic acid it has been shown that cells can survive the transition and enter myogenesis [3].

The genes which will be over expressed or suppressed in this thesis are *MYOD1* and *POU5F1* respectively to induce differentiation of hiPSCs to skeletal myocytes [1].

1.1.4 CRISPR-Cas9

Clustered Regularly Interspaced Short Palindromic Repeat (CRISPR)-Cas technology is a robust method of genome engineering. The method originates from the adaptive immune system of bacteria and archaea, there it protects them from phages [29]. In this thesis, the CRISPR-Cas9 system from *Streptococcus pyogenes* (SpCas9) was applied, it is one of the most commonly used systems. The single-guide RNA enables the SpCas9 to find a specific site in the genome. In figure 1.1 the entire process of genome editing through CRISPR-cas9 is shown. The sgRNA will direct the Cas9 endonuclease to the correct site in the genome and then the nuclease will create a double stranded break in the DNA. After the break is created, cells have four ways to repair the damage, either through non-homologous end joining (NHEJ), homology directed repair (HDR), microhomology-mediated end joining or homology-mediated end joining [29, 30].
SpCas9 can insert, modify or delete parts of the genome with efficiency varying with both cargo and the target locus. A double-stranded break is created by the nuclease, the template DNA is inserted by the break, after which the break is repaired again. In the presence of donor DNA, the donor can be incorporated, without a donor template the cell will try to repair the break primarily through NHEJ [31].
Although the technology comes with a powerful gene editing capability it is not perfect, small insertions and deletions (indels) do occur and the outcome of the editing does not always result in both alleles edited rather it can occur that one allele is edited and the other remains unchanged or is subject to a small insertion or indel [32].

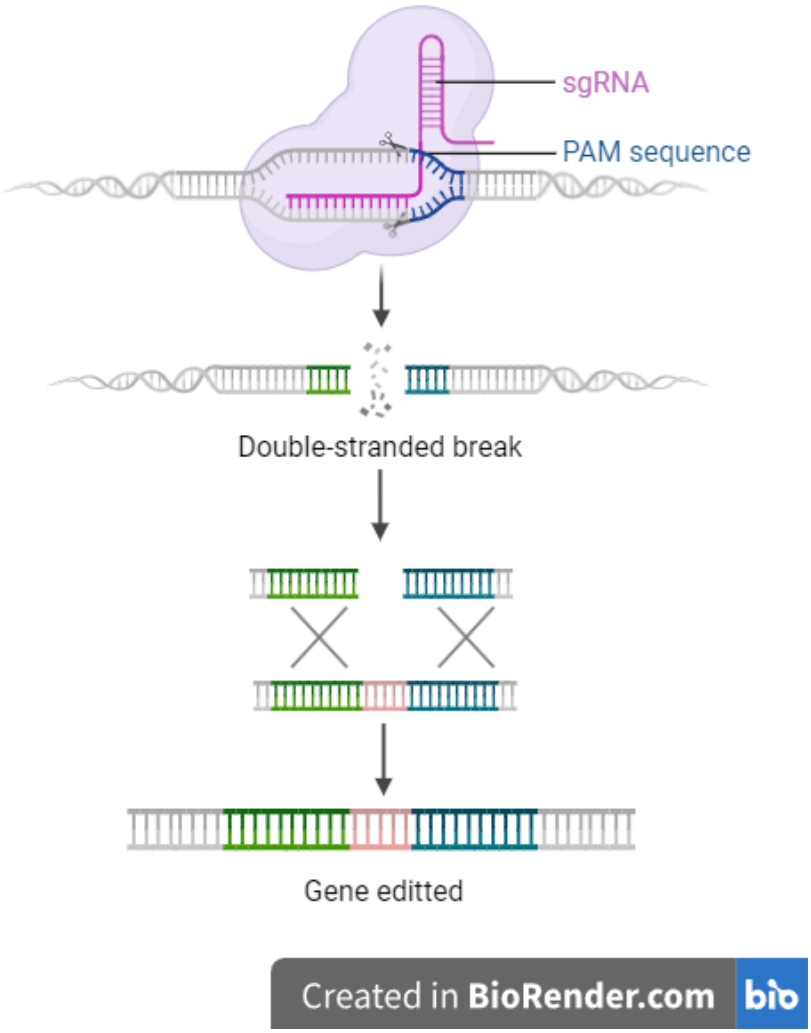

Figure 1.1: CRISPR-Cas9 gene editing, sgRNA guides the endonuclease into place by the PAM sequence and matching the guide to the DNA strand. Homology arms guide the donor to the DNA break and homology directed repair occurs. sgRNA = Single-guide RNA, PAM = protospacer adjacent motif. Image was created in Biorender.

1.1.5 Xential

Xential is a genome editing enrichment method which introduces Diphtheria Toxin (DT) resistance to a population of cells as well as any genes of interest. By a single point mutation in *HBEGF* the cells become resistance to DT while the HBEGF receptor retains all other functions [9]. The genome editing is performed on the third exon of the *HBEGF* receptor gene. The genomic template of choice is inserted downstream of the third exon while the receptor itself is only changed by the point mutation to create resistance to DT. The advantage of Xential is that it only requires a single insertion vector without introducing any other than the genes of interest. The editing strategy will result in a population of either unedited cells, cells with one allele edited or cells with both alleles edited. When exposed to DT only cells without wild-type HBEGF receptors survive (fig. 1.2). As such, Xential results in a cell population with biallelic editing.

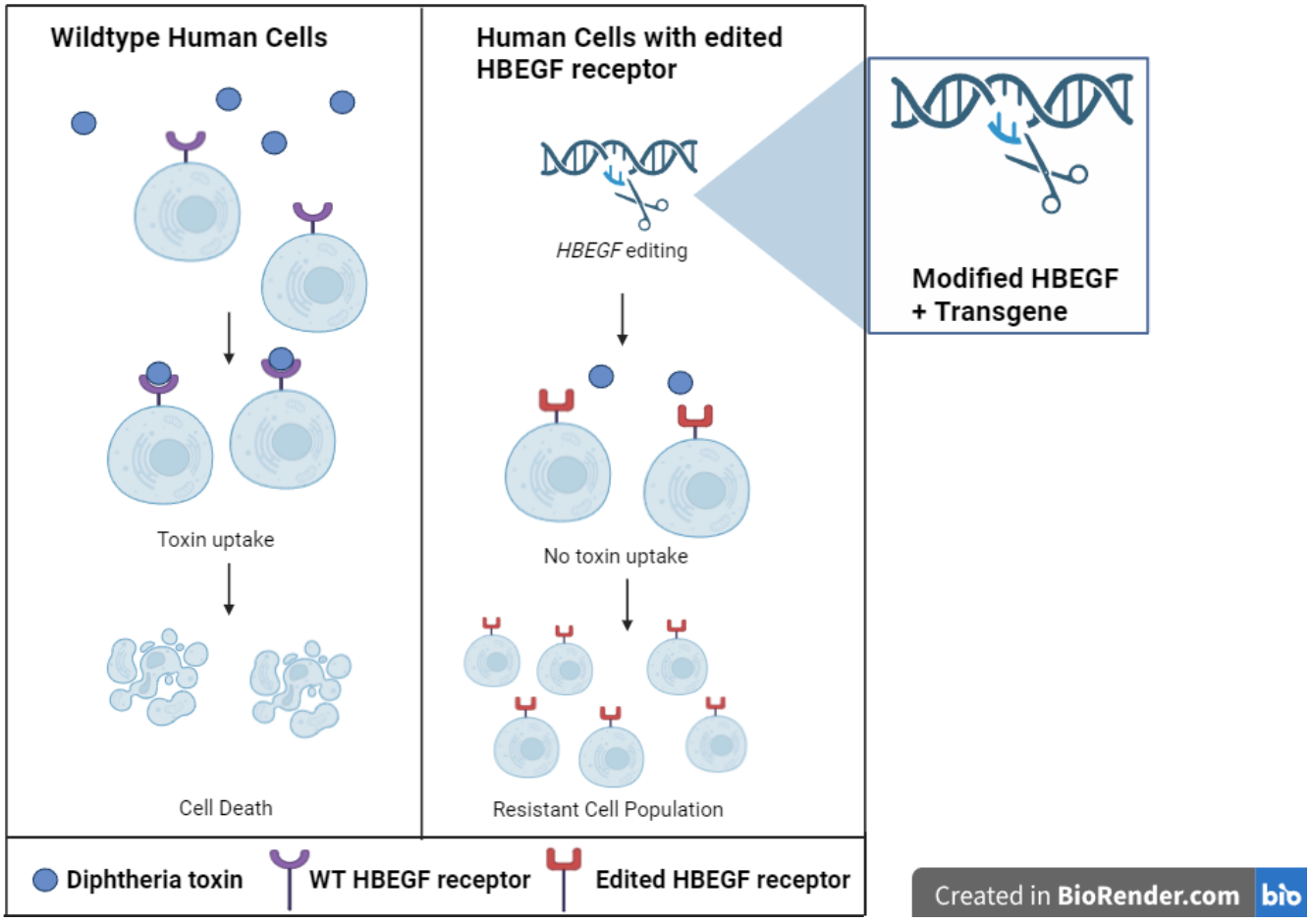

Figure 1.2: Toxin based selection of wild-type (WT) HBEGF cells and edited cells, on the left hand side the diptheria toxin (blue circle) can bind to the HBEGF receptor (purple) and be transported into the cell after which it will inactivate translation elongation factor 2 and kill the cell. On the right hand side the edited HBEGF receptor (red) do not recognize the toxin and it is not transported into the cells leading to cell survival. DT = Diphtheria Toxin, WT = wild-type. Image was created in Biorender.

1.2 Aim

The aim of this thesis was to use Xential to modulate MYOD1 and OCT4 to differentiate hiPSCs into skeletal myocytes. Does direct programming lead to relevant phenotypes of cells when using Xential? Furthermore, could modifying the expression be the key to solving the heterogeneity observed in previous direct programming?

1.2.1 Specific objectives

The thesis aimed generate inducible cell lines that could differentiate into skeletal myocytes by using the Xential method. To be able to achieve this, pluripotency of the cell line was measured through immunofluorescent imaging. The integration and inducibility of the transgenes was assessed, after which an attempt to differentiate the cells into skeletal myocytes proceeded. The differentiated cells were compared to commercially available skeletal myocytes by measurements of flow cytometry, RT-qPCR and immunofluorescent imaging.

1.2.2 Strategy outline

The differentiation of iPSCs into skeletal myocytes consists of several steps (fig. 1.3). First the genes of interest will be introduced through Xential to the cells. Second, the cells will undergo a Diphtheria toxin (DT) selection, where they are treated with the toxin over a period of time to kill off any unedited cells. The doxycycline inducible iPSCs can now be used to acquire skeletal myocytes. This system was chosen to allow for growth of the hiPSCs post-transfection without any unintended differentiation into skeletal myocytes and to allow for unlimited differentiation scale at will. An inducible system will also ensure that in the event of successful integration, further optimisation of the differentiation protocol can proceed without compromising the amount of viable edited hiPSCs that are at hand and the differentiation can occur at an intended time point from the same base cell line.

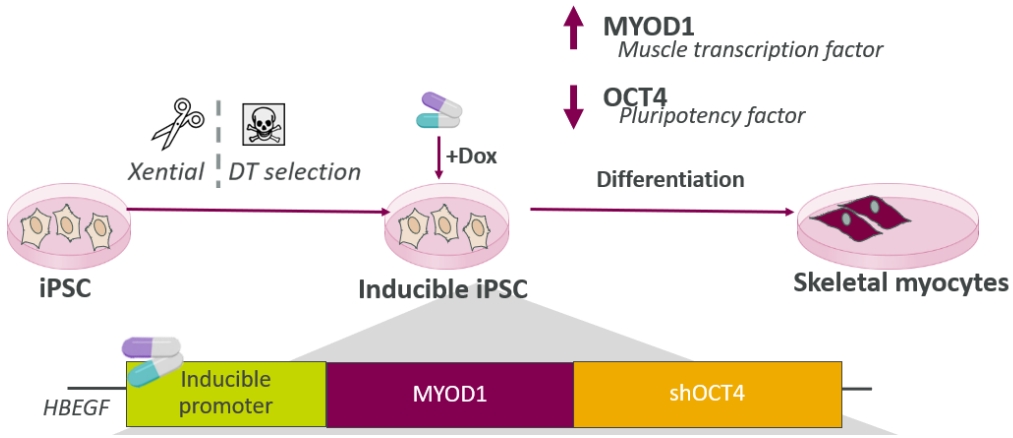

Figure 1.3: The differentiation process using Xential Diphtheria toxin (DT) selection, applying doxycycline will result in an up-regulated MYOD1 and a down regulation of *OCT4* by short hairpin RNA. DT = Diphtheria Toxin, Dox = Doxycyline, iPSC = induced Pluripotent Stem Cells, sh = Short hairpin.

2
Methods

2.1 Cell Culture Conditions

Cells were kept in a BBD6220 CO_2 incubator (Thermo Fisher Scientific) set to 37° C, 5% CO_2, 19.7% O_2 and 95% relative humidity (rH). The cells were maintained in Cellartis DEF-CS 500 system (Takara Bio). Coating, media and growth factors were all prepared according to instructions by the manufacturer.

2.2 Transgenes

There are several different aspects to the genetic cargo that this project aims to integrate into hiPSCs genome. iX was created based on the internal study done previous to this project (fig. 2.1). From left to right, top to bottom, the transcription unit consists of the following. First reverse tetracycline-controlled transactivator 4, rTTA4, which is a modified version of the tTA that will together with Tetracycline Response Element 3rd Generation, TRE3G, constitute an inducible system under the chemical doxycycline [33].

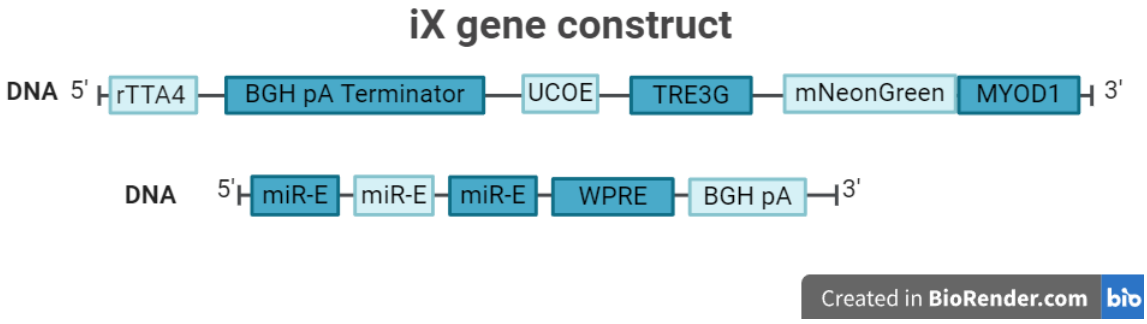

Figure 2.1: All components of the iX transgene in order, the top strand is upstream of the bottom strand. rTTA4 = reverse tetracycline-controlled transactivator 4, BGA pA = bovine growth hormone polyadenylation element, UCOE = Ubiquitous chromatin opening elements, TRE3G = Tetracycline Response Element 3rd Generation, MYOD1 = Myogenic differentiation 1, miR-E = microRNA backbone, WPRE = woodchuck hepatitis virus post-transcriptional regulatory element. Image was created in biorender.

The bovine growth hormone polyadenylation element (BGH pA) is meant to protect the different transcribed genes, in this case the *HBEGF* and downstream the entire

MYOD1 and three different shRNAs (miR-E, a short hairpin backbone shown to increase mature miRNA levels up to 30-fold) [34]. It has been shown that the right choice of polyadenylation tail can increase the expression levels of transgenes significantly [35].
Ubiquitous chromatin opening elements (UCOE) is downstream of the first BGH pA. It has been shown to protect the silencing of genes from epigenetic factors [36]. Downstream of the *TRE3G* promoter, mNeonGreen is coupled with *MYOD1*. The mNeonGreen will act as a fluorescent label to the MYOD1. The production of MYOD1 can then be tracked visually and sorting of cells based on the expression of *MYOD1* can proceed without the need of killing the cells to extract and analyze the proteins or RNA involved [37].

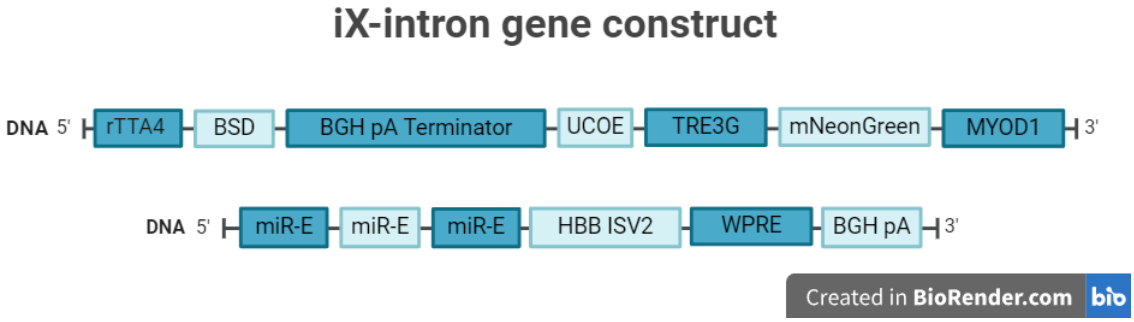

Figure 2.2: All components of the iX-intron transgene in order, the top strand is upstream of the bottom strand. rTTA4 = reverse tetracycline-controlled transactivator 4, BGA pA = bovine growth hormone polyadenylation element, UCOE = Ubiquitous chromatin opening elements, TRE3G = Tetracycline Response Element 3rd Generation, MYOD1 = Myogenic differentiation 1, miR-E = microRNA backbone, WPRE = woodchuck hepatitis virus post-transcriptional regulatory element. HBB ISV2 = Hemoglobin Subunit Beta, Intervening Sequence 2. Image was created in biorender.

The woodchuck hepatitis virus post-transcriptional regulatory element (*WPRE*) has been shown to increase transgene production and works best when placed close to the polyadenylation tail. Lastly iX ends with a polyadenylation tail for the produced transcription factors and short hairpins. To increase the expression of *MYOD1* and the shRNA, a new construct with an intron sequence, iX-intron was created (fig. 2.2. The intron sequence "Hemoglobin Subunit Beta, Intervening Sequence 2", HBB IVS2, has been shown to increase RNA production from 2-fold up to 500-fold by supporting mRNA splicing, was placed upstream of the poly A tail element[38]. Apart from the HBB IVS2 intron sequence, Blasticidin S deaminase (BSD) was added upstream of the first BGH to allow for further selection through Blasticidin if the homogeneity is not achieved through increased expression levels of *MYOD1* and the shRNA targeting *POU5F1* [39]. Lastly as a reference, a construct with only a point mutated *HBEGF* was used as a control for all experiments post transfection.

2.3 Purification of Plasmids

The plasmids which were to be integrated into the genome of the hiPSCs were ordered from Genscript. The plasmids were transformed into *Escherichia coli* as follow: Competent *E. coli* were thawed on ice, the cells were then heat shocked in a water bath set to 42° C for 30 sec. After incubating the cells on ice for 2 minutes, 300 μl of HB (heart infusion broth) media was added and the cells were left to incubate at 37° C for one hour. The cells were then spun down at 3000rpm for 5 minutes, resuspended in 100 μl of HB media and plated on agar plates containing appropriate antibiotic for each plasmid. The transformed *E. coli* were grown overnight in 37° C after which single colonies were selected to grow in 3 mL HB media with antibiotics added. The cells were grown overnight in 37° C, 220 rpm. The antibiotics were Kanamycin disulfate (Sigma Aldritch) and Carbenicillin disodium salt (Sigma Aldritch) each at a final concentration of 100 μg/mL. Purification of the plasmids from the *E.coli* was performed using a midiprep kit from Qiagen. A full map of the plasmids can be found in Appendix A.

2.4 Transfection

Reverse transfection of hiPSCs was performed using FuGene HD from Promega and used according to instructions. Cas9 plasmid was added at 125 ng, *HBEGF* sgRNA at 40 ng and HBEGF donor at 235 ng per 6 well per reaction. The transfection was performed 24 hours after splitting cells in order to transfect during the log phase of the cell's growth.

2.5 Diphtheria toxin selection

After growing the transfected cells up to confluent, DT-selection was performed for 96 hours. The media was refreshed daily with new growth factors and DT at 10 μg/mL concentration. After the DT-selection, the cells were kept in culture until confluent or until growth was hindered by lack of fresh coating material on the plate. In both cases the cells were split and scaled up to larger plates to accommodate for future experiments.

2.6 Differentiation of iX and iX-intron

For differentiation of Xential edited hiPSCs to skeletal myocytes, a media consisting of high glucose DMEM with l-glutamine (4500 mg/L Glucose, GibCo Thermo Fisher Scientific) , 1x Insulin-Transferrin-Selenium (GibCo Thermo Fisher Scientific), 10% Knockout Serum Replacement (Thermo Fisher Scientific) and 1x N-2 supplement (GibCo Thermo Fisher Scientific) was used. The media was supplemented fresh with 1 μg/mL Doxycycline during each media change. During seeding the media was also supplemented with Rock inhibitor Y-27632 (Stem Cell Technologies) at 10μM. Plates were supplied by CORNING and whre coated using Geltrex (Thermo fisher

scientific) diluted 1:100 in DMEM-F12 (Thermo fisher scientific). Media changes were performed daily for the first three days after which it was performed every other day. The cells were kept in culture for a total of seven days.

Table 2.1: Amount of cells for 6 well or 96 well plates with corresponding factors at the top of each column. Unless otherwise specified, fraction 1 was used.

Well	1	3/4	2/4	1/4
6	800 000	600 000	400 000	200 000
96	35 000	26 250	17 500	8750

The seeding density was 800 000 cells per 6 well, 35000 per 96 well. Fractions of this was cultured for one cell line, 26500, 17500, 8750 cells per 96 well and 600 000, 400 000, 200 000 cells per 6 well.

2.7 Incucyte Analysis

The incubator (Thermo Fisher Scientific) was set to 37° C, 5% CO_2. rH and O_2 was not regulated by the incubator. Phase imaginging and mNeonGreen imaging was performed every 2 hours. The incucyte SX5 (Sartorius) was set up as follows: Basic Analyzer, Standard Scan, Phase and Green channel (300 ms acquisition) imaging at 10x magnification, Green Channel Unit threshold was set to 0.2, confluency was calculated through the AI confluency tool. Phase confluency and "Green confluency / Phase Confluency" was exported from the incucyte and analyzed in GraphPad Prism 9.

2.8 Flow cytometry

Cells were harvested the day prior to running the flow cytometry and prepared by washing them with phosphate buffered saline pH 7.4 without magnesium, calcium, and phenol red, (PBS, Thermo Fisher Scientific), centrifuging at 300g for 5 minutes, resuspended in fixation buffer (R&D systems), 100 μl per 1 million cells. The pellet was resuspended to prevent cross-linking of individual cells. After fixating at room temperature for 10 minutes the cells were again washed with PBS and centrifuged at 300g for 5 minutes. The cells were resuspended in 100 μl of Cell permeabilization buffer (0.1% Triton-X, 1 percent Blocker BSA, PBS, Thermo Fisher Scientific) per 1 million cells and incubated at room temperature for 10 minutes. Cells were separated according to the needs of each flow cytometry and stained with primary antibodies in 100 μl blocking buffer (1% Blocker BSA , PBS, Thermo Fisher Scientific) overnight at 4° C. On the day of the flow cytometry, cells were washed with blocking buffer and spun down at 300g for 10 minutes. The supernatant was discarded, and the secondary antibodies were added along with blocking buffer and left to incubate for 1 hour at room temperature. Each sample was then centrifuged at 300g for 10 minutes, the supernatant was discarded, and all samples were resuspended in 100 μl

blocking buffer each to be analyzed in a BD FACS Symphony A1 (BD Bioscience). In table 2.2 a full overview of each stainings is presented. For cells analyzed for only mNeonGreen, no staining was used.

Table 2.2: An overview of the antibodies used in flow cytometry experiments. The amount indicated is per 100 μl of blocking buffer that cells were resuspended in.

Target	Species	Amount (μl)	Product Number	Company
MYOD1	Rabbit	2	#13812	Cell Signaling Technologies
MYH1	Rabbit	2.5	MF20	DSHB
IgG1	human	2	PE, REA293	Miltenyi Biotec
Anti-rabbit	Donkey	0.25	A10042	Life technologies

FlowJo was used to analyze all flow cytometry data, gating was performed to identify cell populations. The full gating strategy is shown in appendix A. FlowJo's own normalisation to counts method was used to account for different number of cells between samples.

2.9 Reverse transcriptase qPCR

Cell lines were harvested and RNA was extracted from the cells using an All-Prep DNA/RNA Micro kit (Qiagen) according to instructions. cDNA was created through the High-Capacity cDNA Reverse Transcription Kit (Thermo Fisher Scientific) according to the instructions included in the kit. qPCR reactions were conducted with 20 ng of cDNA per reaction. Probes were used for three housekeepers, TATA-Box Binding Protein (*TBP*), Glyceraldehyde 3-phosphate dehydrogenase (*GAPDH*) and Actin Beta (*ACTB*). The genes that were probed were Desmin (*DES*), Octamer-Binding transcription factor 4 (*POU5F1*), Myogenic differentiation 1 (*MYOD1*), Myocyte enhancer factor 2C (*MEF2C*) and Myogenin (*MYOG*). The qPCR was performed with the TaqMan Real Time PCR mastermix (Thermo Fisher Scientific) and the probes were also of TaqMan (Thermo Fisher Scientific). RT-qPCR was performed in a QuantStudio Flex 7 (Applied Biosystems by Thermo Fisher Scientific), using the QuantStudie Real-Time PCR software. The settings for the RT-qPCR runs were: 40 cycles of 95° C for 20 sec, 60° C for 20 secs. Using the Fast program, FAM as reporter and it was conducted as a comparative CT. Each reaction was performed with 10 μl.

2.10 Immunofluorescence imaging

Cells were fixated by removing the media, washing with PBS, adding 4% PFA, incubating at room temperature for 20 minutes and then washing twice with PBS to then be sealed and stored at 4° C. The day before imaging, PBS was removed and blocking buffer (0.1% Triton-X, 1% Blocker BSA, PBS) was added to incubate for an hour at room temperature, the cells were washed once with PBS then primary

antibodies in blocking buffer was added to incubate over night at 4° C. In table 2.3 the compounds used to stain the fixated cells is shown.

Table 2.3: An overview of the antibodies used in immunofluorescence experiments. The amount indicated is per 100 μl of blocking buffer that cells are resuspended in.

Target	Species	Amount (μl)	Product Number	Company
OCT4	Rabbit	3	#2750	Thermofisher
MYOD1	Rabbit	1.5	#13812	Cell Signaling Technologies
DESMIN	Rabbit	3	#5332	Cell Signaling Technologies
MYOG	Rabbit	6	ab124800	Abcam
Anti-rabbit	Donkey	1	A10042	Life technologies

On the day of imaging, the cells were washed twice with PBS and then secondary antibodies and cell stains were added to incubate for an hour at room temperature. HCS CellMask-Deep Red or Phalloidin-488 (Thermo Fisher Scientific) were used as cellular stains and hoechst was used to stain the nuclei of the cells. After the incubation the cells were washed twice with PBS and then covered in fresh PBS to be sealed with a black plastic film. Imaging was performed using a YOKOGAWA 7000 according to the manufacturer's instructions. Each well was imaged at five different places and optimization of camera distance was performed prior to each imaging when using a different plate.

2.11 Skeletal Myocyte Commercial kits

Each commercial kit was seeded and treated as per the instructions of the supplier. For Amsbio, plates were coated with Collagen type 1 rat tail (Thermo Fisher Scientific) diluted in PBS rather than using precoated plates. The BitBio cells (ioSkeletal Myocytes) were cultured on plates coated with Geltrex (Thermo fisher scientific) diluted in 1:100 DMEM-F12.

2.12 Statistics

GraphPad Prism 9 was used for statistical testing, the inbuilt function to conduct 2-way ANOVA analysis with multiple comparisons was used. RT-qPCR data was first normalized to three housekeeper genes within each sample, *GAPDH*, *TBP* and *ACTB*, after which data for overexpression was normalized to the same cell lines *TBP* and data for silencing of genes was normalized to the *HBEGF* control cells. The data was then put into GraphPad Prism 9 to be visualized and statistically tested. For flow cytometry, FlowJo was used to analyze results as described in methods 2.8.

3

Results

The result section is divided up into several parts, first the generation of the cell lines will be presented in chronological order. Secondly, attempts to differentiate skeletal myocytes from the generated cell lines will be presented. Lastly, a commercial skeletal myocytes differentiation kit will be presented to establish a comparison.

3.1 Generation of Cell Lines

There are several steps involved in the generation of cell lines. IPSCs were validated for pluripotency as the end goal was to differentiate them. Transfection of the transgenes could then proceed and Diphtheria toxin selection was used to eliminate any wild-type cells left in the population. Inducibilty and growth rate of the generated cell lines was then tested.

3.1.1 Pluripotency Validation of iPSCs

New cell lines aimed to differentiate require confirmation that there are induced pluripotent stem cells present prior to modifying them. The pluripotency of the iPSCs was confirmed through IF imaging where OCT4 was found in the cell nuclei overlapping with Hoechst (fig. 3.1). All cells present in the images were positive for OCT4 as is confirmed in fig. 3.1 c where all cell nuclei are purple.

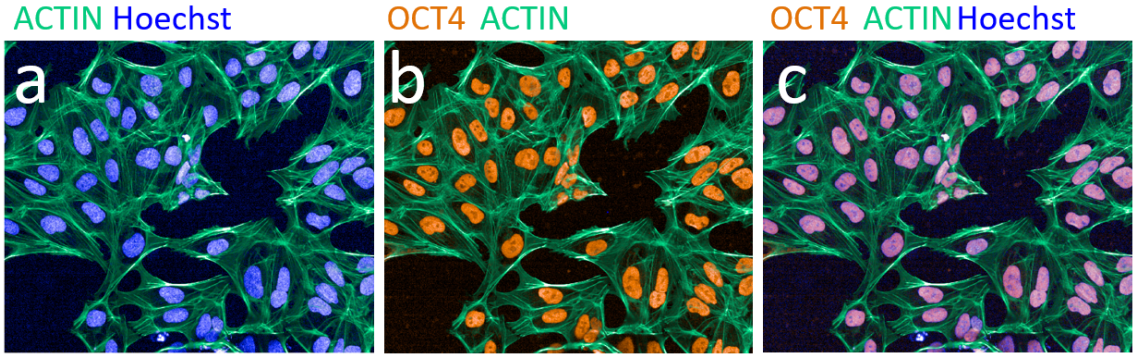

Figure 3.1: Wild-type iPSCs stained for hoechst (blue, cell nuclei stain), OCT4 (orange), ACTIN (Green) and are shown as indicated above each image. Images were captured with a YOKOGAWA 7000.

3.1.2 Diphtheria toxin selection of Xential edited iPSCs

After insertion of the transgenes, the cells were grown to confluency before being exposed to Diphtheria toxin (DT). Five days post DT selection, cell line survival was investigated through phase imaging (fig. 3.2). Each cell line with edited *HBEGF* survived the selection. There are differences in confluency between the cell lines. iX-intron had three distinct colonies growing while iX had one visible colony in the well. The *HBEGF* control cell line which had no genetic cargo other than the point mutated *HBEGF* shows the highest confluency across all four cell lines. The wild-type control which, in this case, was only adding sgRNA and SpCas9, shows no signs of life. The wild-type control continued to show no cells for another two weeks before being discarded. The wild-type control was included to see if SpCas9, with the *HBEGF locus* as a target, would incur any indels or modification which could lead to DT selection survival (fig. 3.2).

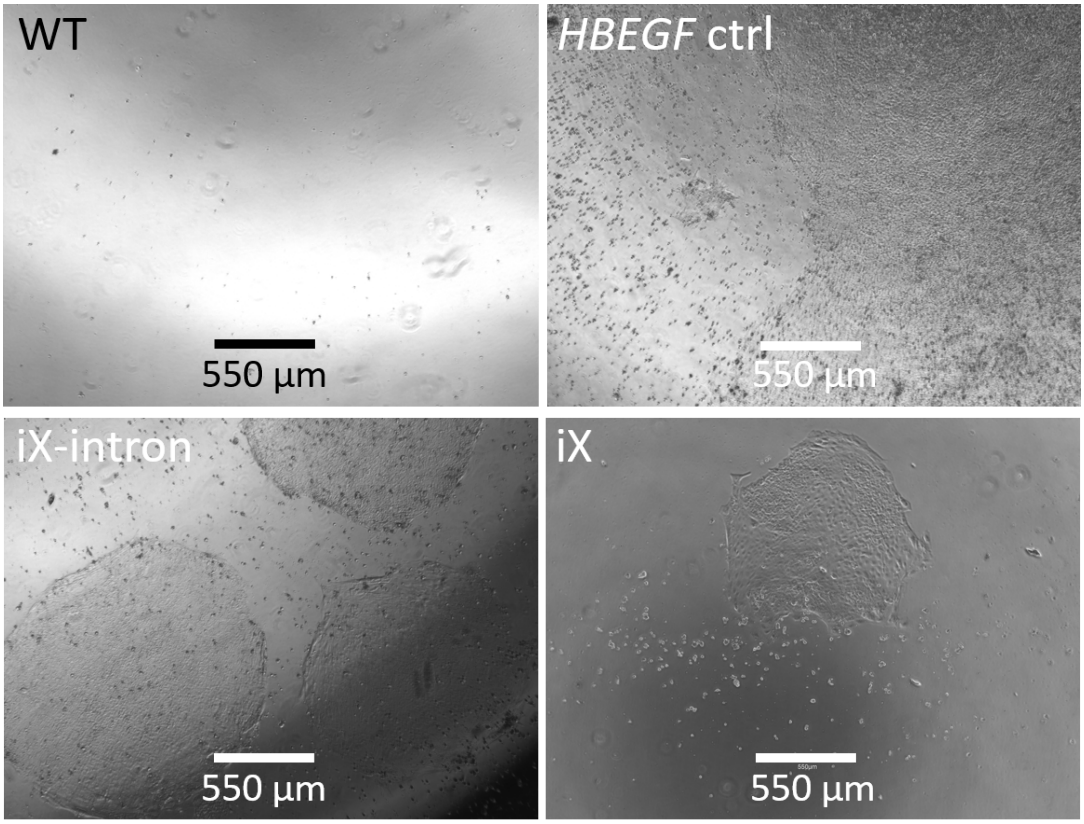

Figure 3.2: Diphtheria toxin selected cells t=5 days post selection, wild-type control, *HBEGF* control, iX-intron and iX as indicated in the images. The white/black bar in each image indicates 550 μm. WT = wild-type. Images were acquired using the phase lens of an Invitrogen EVOS FL Digital Inverted Fluorescence Microscope.

3.1.3 Doxycyline Induction

Incorporation of the inserts and doxycycline responsiveness of iX and iX-intron was verified through doxycycline induction in an incucyte (fig. 3.3). The expression of mNeonGreen coupled to MYOD1 was tracked through the fluorescence of mNeonGreen. For all time points, cells treated with doxycycline for both iX and iX-intron show a significant increase in mNeonGreen area / phase area, only one comparison is shown in each subfigure of figure 3.3 to keep them readable. There was no significant difference observed between both control conditions and the transgenic cell lines treated with 0 μg/mL doxycycline.

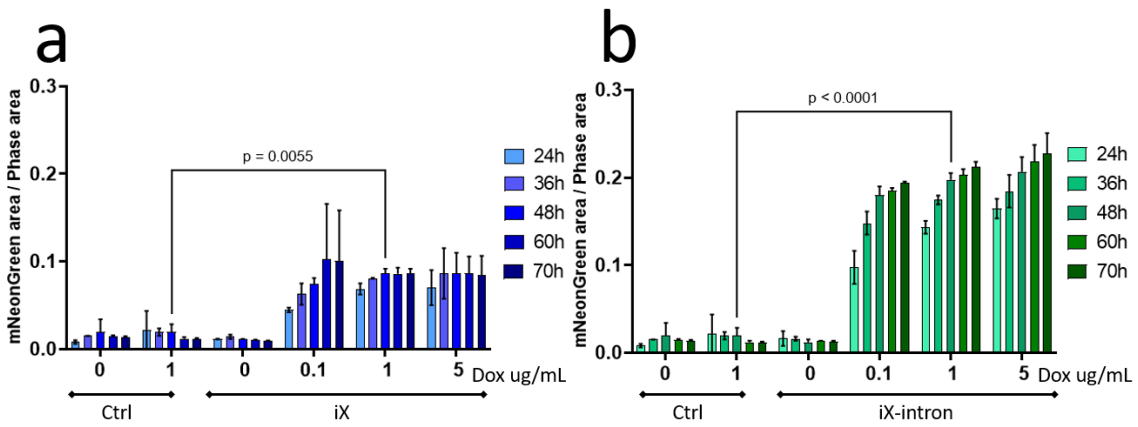

Figure 3.3: mNeonGreen area / phase area of live cells incubated for 70 hours in an incucyte. Measurements at 24, 36, 48, 60 and 70 hours are shown next to each other for each level of doxycycline. The deepening of the colour indicates increasing amount of time passed since the initiation of the induction. Doxycycline is shown in levels of μg/mL indicated on the x-axis. Each control had three replicates and each doxycycline level for iX (a) and iX-intron (b) had two replicates. Statistics was performed using a 2-way ANOVA table with multiple comparisons between each time point and condition (only two shown at 48 hours between 1 μg/mL doxycycline for the ctrl, iX and iX-intron). Dox = Doxycycline, ctrl = *HBEGF* control, h = hours.

Growth rate with and without doxycycline was also investigated. It was found that iX had a significantly decreased growth rate compared to the *HBEGF* control cell line at 58 hours after seeding when treated with 1 μg/mL of doxycycline (fig. 3.4). There were no other significant changes in growth rate with or without doxycycline.

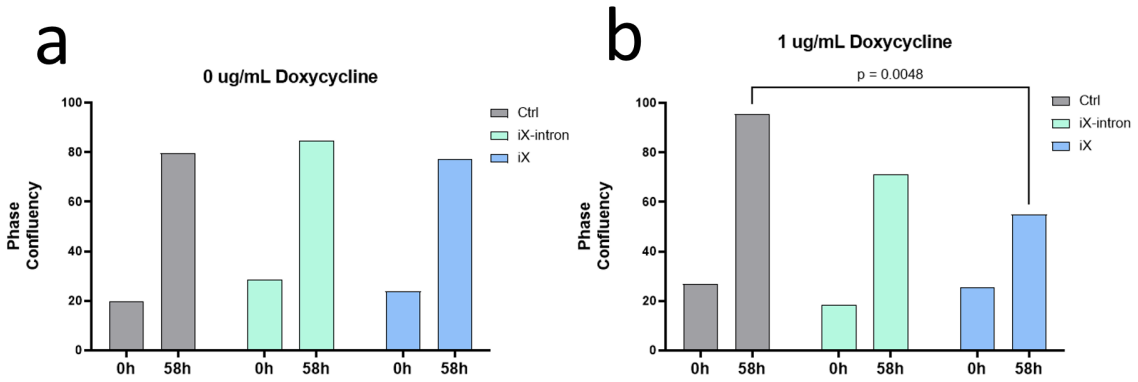

Figure 3.4: Phase confluency (y-axis) of *HBEGF* control (grey), iX-intron (teal) and iX (blue) at 0 hours and 58 hours (indicated on the x-axis). Doxycycline concentrations at 0 and 1 μg/mL as indicated in each image. Statistical analysis was performed through a 2-way ANOVA table with multiple comparisons, only the significant comparisons are shown in the figure. h = hours, Ctrl = *HBEGF* control

3.1.4 Quantifying cell lines response to doxycycline through flow cytometry

To investigate how homogeneously the response of each doxycycline induced cell line was, fluorescence activated cell sorting was performed on the cells induced in the previous section 3.1.3. The gate for positive mNeonGreen cells was placed so that it includes none of the untreated wild-type cells (not displayed in the figure), the complete gating strategy is shown in appendix A. At least 50% iX or iX-intron cells were positive for mNeonGreen at all levels of doxycycline treatments. Notably, at 0.1 μg/mL of doxycycline iX exhibited 3.8% more cells positive for mNeonGreen than iX-intron. Conversely, at higher doxycycline concentrations, the iX-intron line demonstrated a higher proportions of mNeonGreen positive cells. Specifically, iX-intron had 26% more cells shifted compared to iX at 1 μg/mL of doxycycline and at 5 μg/mL of doxycycline iX-intron had 21.5% more positive cells than iX.

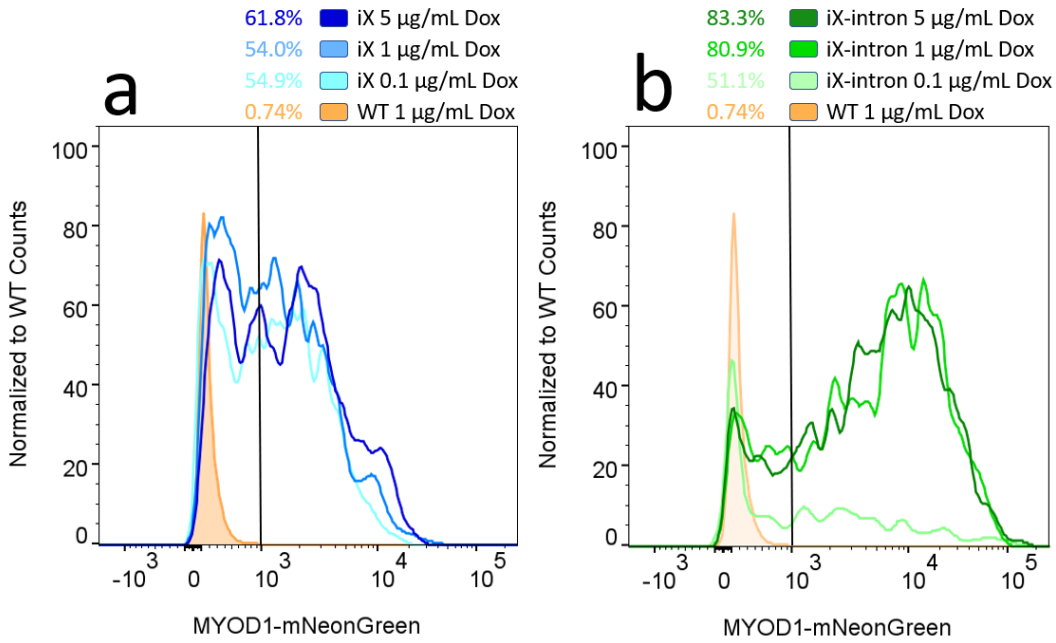

Figure 3.5: FACS results analyzed in FlowJo where two replicates of each Dox condition is represented in the figure (only one is shown). **a**) Three different Dox conditions of iX in blue, percentages shown are the proportion of cells positive for mNeonGreen for each condition. WT cells treated with 1 μg/mL of Dox is shown in orange. **b**) Three different Dox conditions of iX-intron in green, percentages shown are the proportion of cells positive for mNeonGreen for each condition. WT cells treated with 1 μg/mL of Dox is shown in orange. The black vertical lines indicates when cells are positive for mNeonGreen for both **a** and **b**. The experiment was run after the incubating the cells in doxycycline for t=70h. X-axis is measured levels of mNeonGreen coupled to MYOD1 through the AlexaFluor 488 channel. Flow cytometry results were analyzed in FlowJo, WT = wild-type, Dox = Doxycycline.

3.2 Differentiation of Generated Cell Lines into Skeletal Myocytes

The previous sections findings lay a foundation for the exploration of iX and iX-introns ability to differentiate into skeletal myocytes. Having confirmed the pluripotency, validated the inducibility and integration of the inserts, the next step is to subject the cells to their final task, differentiation into skeletal myocytes. The end goal is to asses whether the cell lines express the right markers and assume the desired phenotype.

3.2.1 Phase imaging differentiation of iX and iX-intron

Phase imaging of the differentiation was acquired, after day 5 iX and iX-intron are visibly different. iX showed an elongated pattern with cells aligned with each other. iX-intron had formed dense clusters of cells (fig. 3.6).

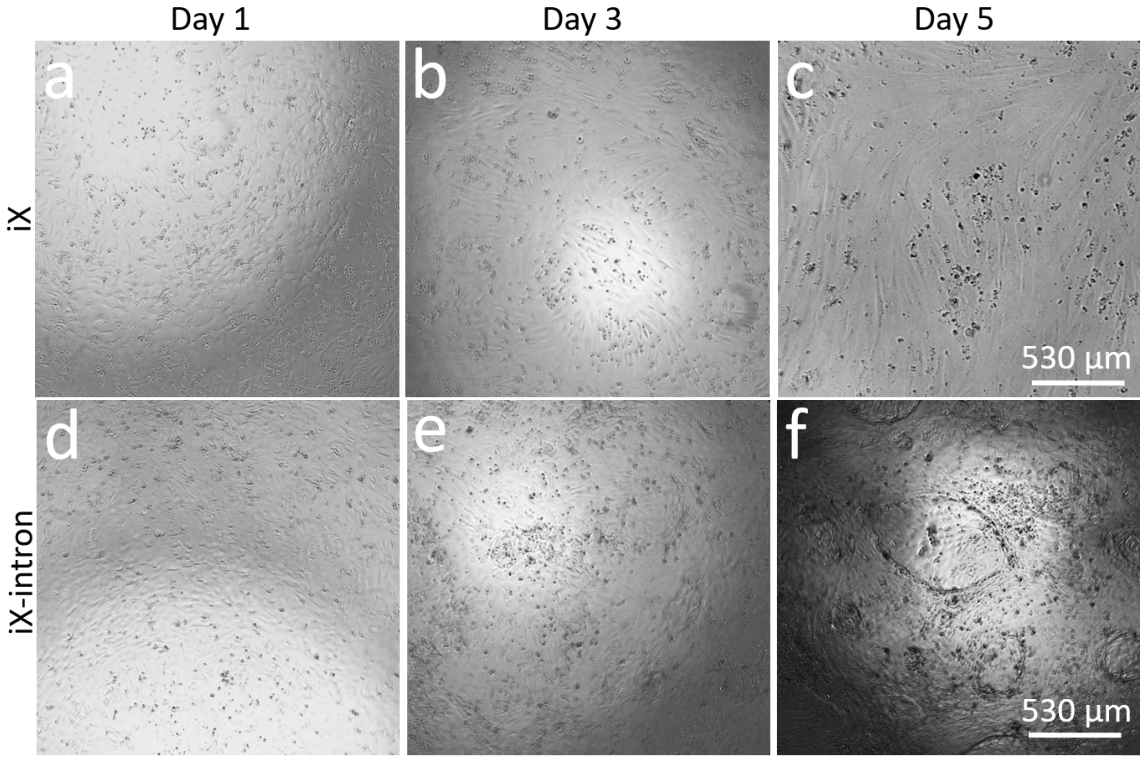

Figure 3.6: Phase images of cells in differentiation media seeded on 96 well plates. **a**) iX 1 day after seeding. **b**) iX 3 days after seeding. **c**) iX 5 days after seeding. **d**) iX-intron 1 day after seeding **)** iX-intron 3 days after seeding. **f**) iX-intron 5 days after seeding. The white bar in **c** and **f** indicates 530 μm. Images were acquired using the phase lens of an Invitrogen EVOS FL Digital Inverted Fluorescence Microscope.

3.2.2 Homogeneity through immunofluorescence imaging

The aim of the immunofluorescence imaging is to visualize the distribution of mNeonGreen, MYOD1, OCT4 and DES within the differentiated cells. DES is tracked

because it is a downstream marker of myogenesis, indicating whether or not the cells have started to commit to becoming skeletal myocytes.

MYOD1 staining on differentiated iX cells was found in the nuclei of several cells in the well although as shown through the CellMask not all cells were positive for MYOD1 (fig. 3.7). iX-intron showed a larger amount of cells positive for MYOD1 and also clustering as observed in the phase imaging (fig. 3.6).

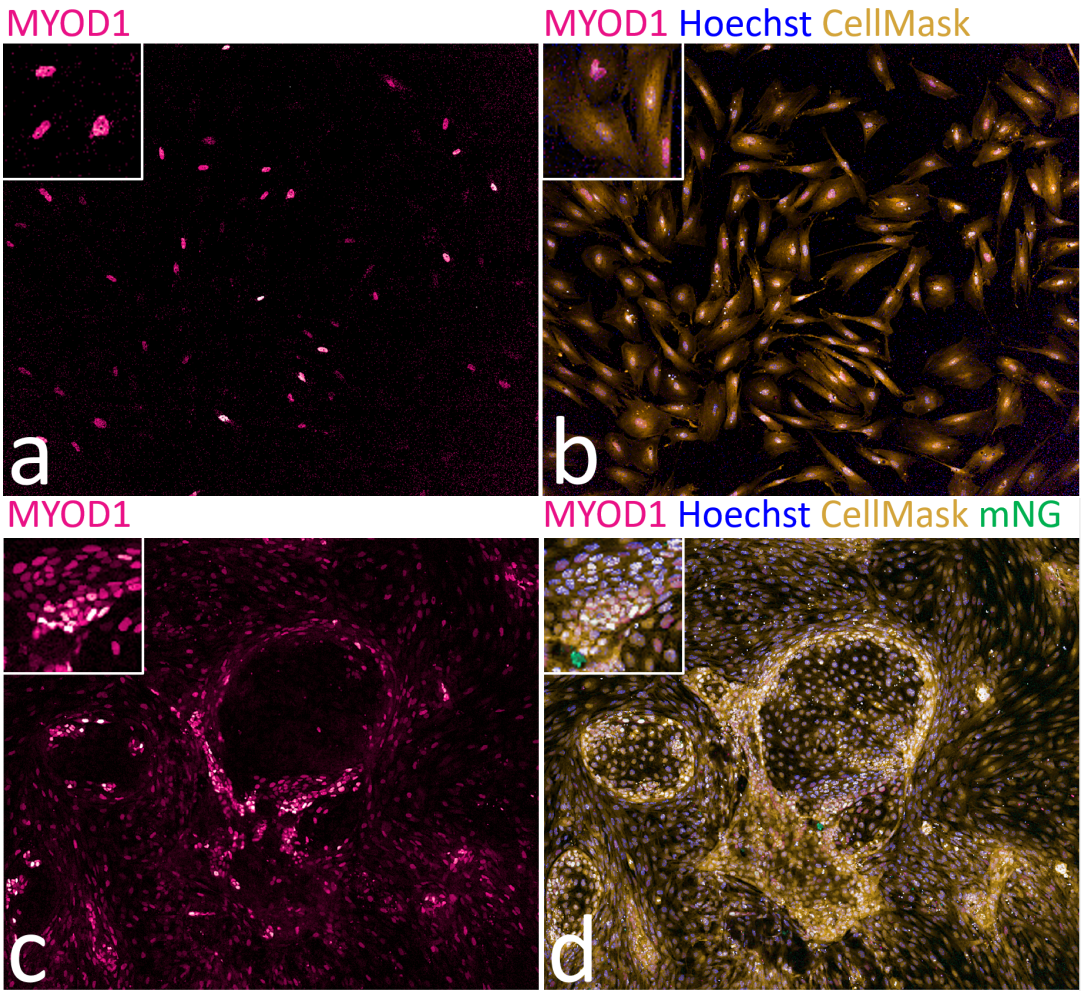

Figure 3.7: Differentiated iX (**a** and **b**) and iX-intron (**c** and **d**) stained for hoechst (blue), CellMask (Yellow) and MYOD1 (Pink), shown as indicated in the images. mNeonGreen is also shown in **d** CellMask = HCS CellMask-Deep Red, MYOD1 = Myogenic Differentiation 1, mNG = mNeonGreen Cells were fixated on the sixth day of differentiation. Images were captured with a YOKOGAWA 7000, uploaded and analyzed in Columbus.

mNeonGreen was not visibly present in iX cells however iX-intron had several cells positive for mNeonGreen with a stronger signal from cells in the clusters (fig. 3.8). Notably, OCT4 was not present for iX and the Cellmask exhibited cells present in the entire image. OCT4 was found in the cell clusters of iX-intron, when OCT4 was overlayed with mNeonGreen the clusters were shown to consist of cells strongly expressing OCT4 and mNeonGreen.

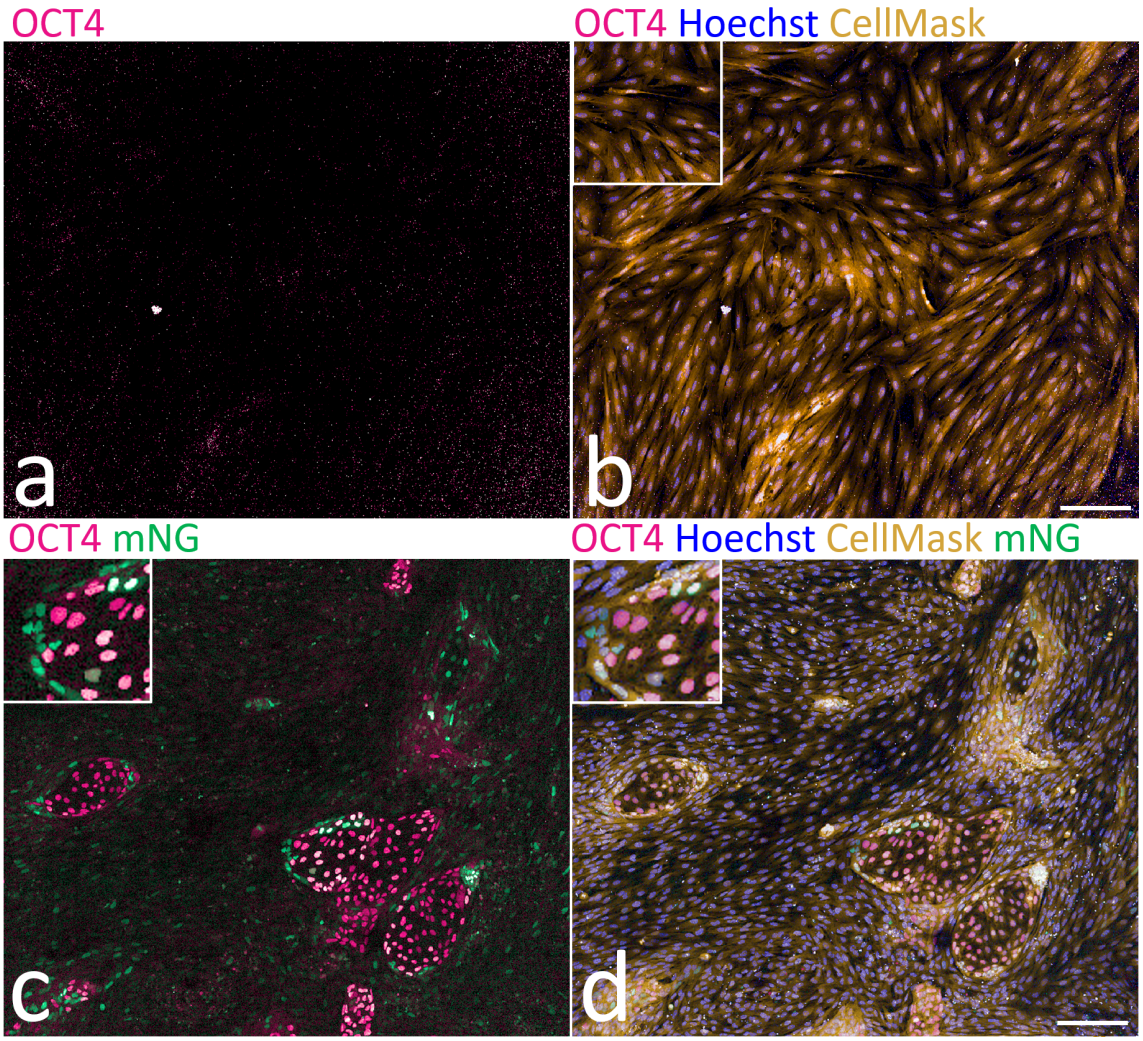

Figure 3.8: Differentiated iX (**a** and **b**) and iX-intron (**c** and **d**) stained for hoechst (blue), CellMask (Yellow) and OCT4 (Pink), shown as indicated in the images. mNeonGreen is also shown in **c** and **d** CellMask = HCS CellMask-Deep Red, OCT4 = Octamer-binding transcription factor 4 , mNG = mNeonGreen Cells were fixated on the sixth day of differentiation. Images were captured with a YOKOGAWA 7000, uploaded and analyzed in Columbus.

DES was present in both iX and iX-intron, notably iX-intron showed DES in a wider spread of cells in the images, neither had DES fully overlapping with the CellMask (fig. 3.9). DES was located in the cytoplasm of the cells for both iX and iX-intron. iX-intron exhibits varying levels of DES as is observed through the nuances in brightness of the DES colouring.

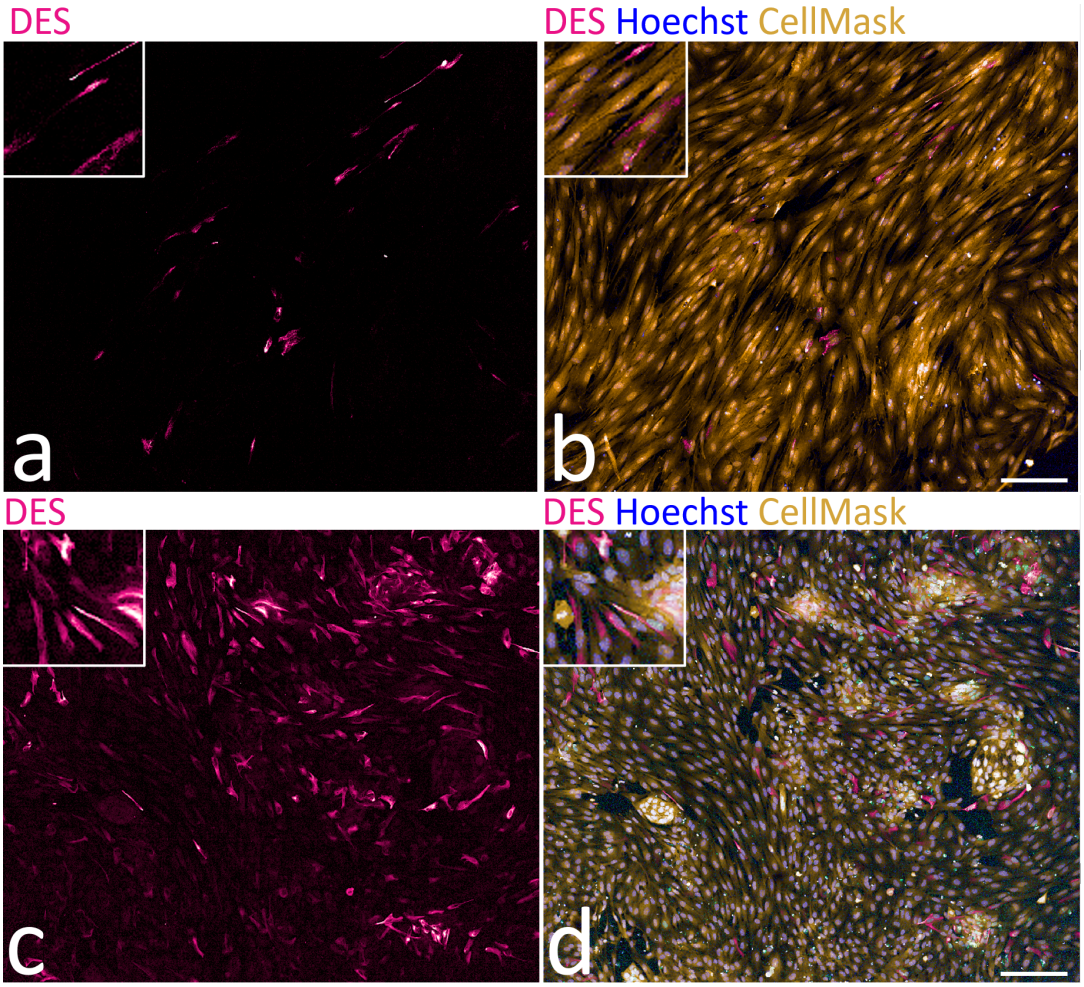

Figure 3.9: Differentiated iX (**a** and **b**) and iX-intron (**c** and **d**) stained for Hoechst (blue), CellMask (Yellow) and DES (Pink), shown as indicated indicated in the images. mNeonGreen is also shown in **c** and **d** CellMask = HCS CellMask-Deep Red, DES = Desmin , mNG = mNeonGreen Cells were fixated on the sixth day of differentiation. Images were captured with a YOKOGAWA 7000, uploaded and analyzed in Columbus.

3.2.3 Quantifying gene and protein expression of differentiated cells

Immunofluorescence imaging does not allow for quantifiable results of how many of the cells are expressing proteins of interest nor to what level the genes are expressed. Therefor flow cytometry and RT-qPCR were conducted.

iX and iX-intron both exhibit a higher mNeonGreen expression than the *HBEGF* control, 99.9% of iX cells are positive for mNeonGreen. Although only 96.2% of iX-introns population demonstrate an expression of mNeonGreen, the majority of the cells are expressing it stronger than the iX cells (fig. 3.10).

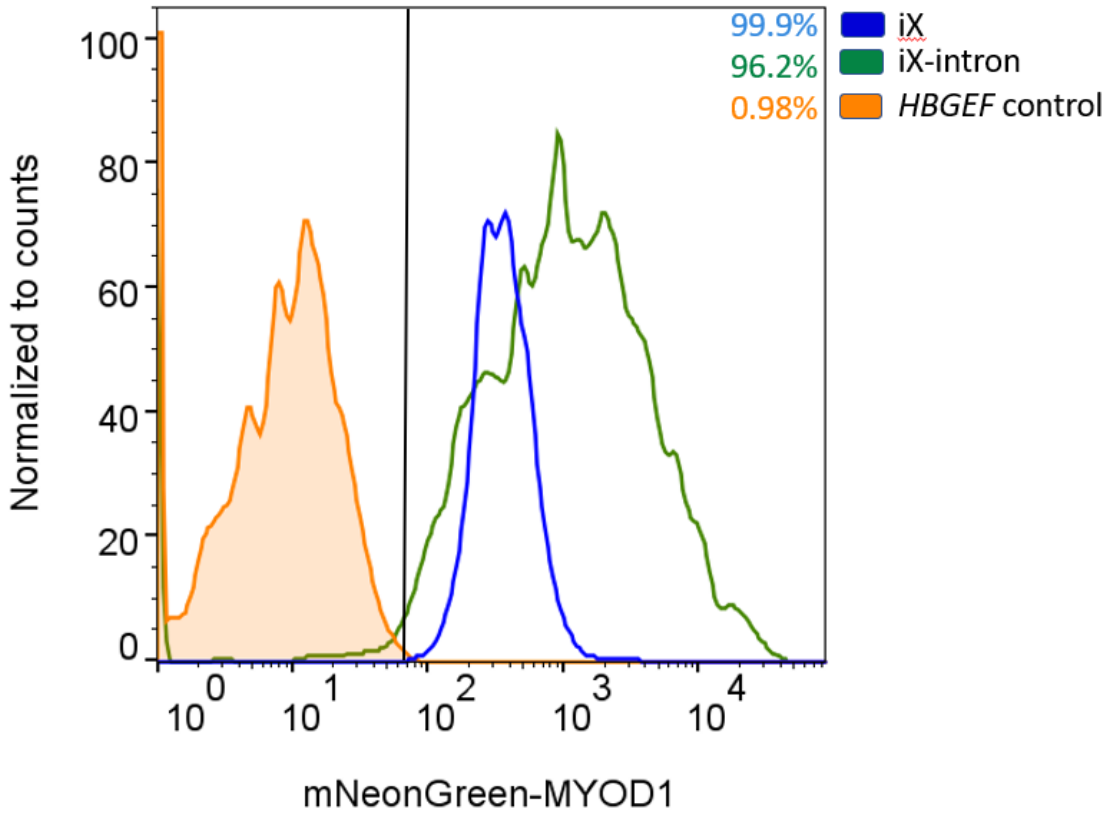

Figure 3.10: FACS results analyzed in FlowJo. iX shown in blue, iX-intron shown in green. Percentages indicate proportion of cells positive for mNeonGreen coupled to MYOD1. The cells were differentiated over the course of 6 days and then fixated. Data was acquired using a FACS Symphony A1 and the mCherry channel. X-axis is measured levels of mNeonGreen coupled to MYOD1 through the AlexaFluor 488 channel. Y-axis is percentage of total counts of cells. The data was normalized through FlowJo to total counts of cells for each cell line. MYOD1 = Myogenic Differentiation 1.

MYOD1 did not show as high a proportion of positive cells for neither iX nor iX-intron. 96.2% of iX were positive for MYOD1 whereas iX-intron had only 59.8% of it's population positive however the gate was set less restrictively due to the peaks not being fully separated from the *HBEGF* control (fig. 3.11b)

Looking at the expression of the downstream marker Myosin Heavy Chain 1, MYH1, will indicate how many of the cells have started to commit to becoming skeletal myocytes. For MYH1 the gating was set as for MYOD1, no more than 10% of the *HBEGF* control was allowed to be positive. Under these circumstances, 81.5% of iX cells were positive for MYH1. Only 52.5% of iX-intron cells were positive with this gating (fig. 3.11a).

For both MYOD1 and MYH1 the iX population was shifted further away from the gate and the *HBEGF* population.

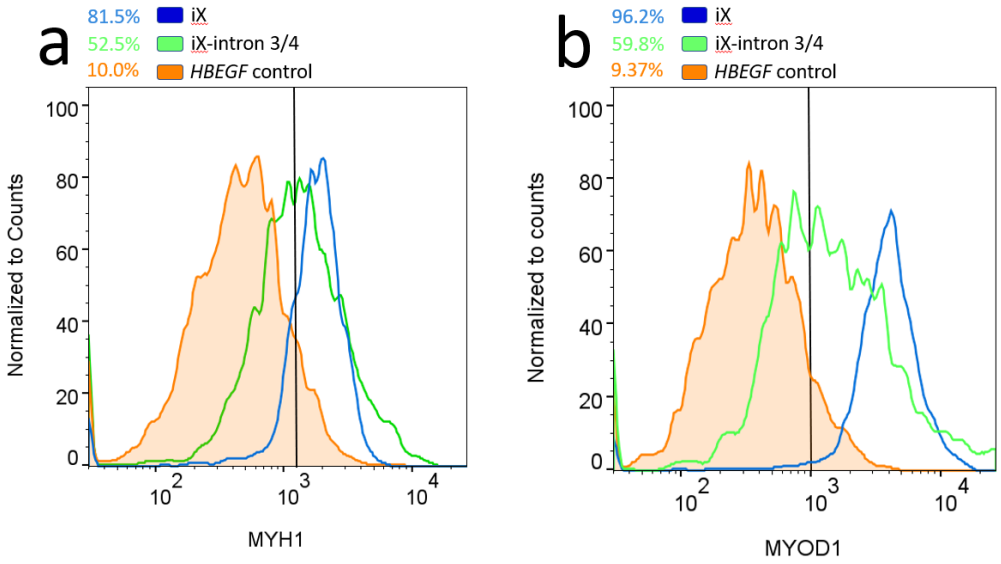

Figure 3.11: FACS results analyzed in FlowJo. iX shown in blue, iX-intron shown in green. *HBEGF* control in orange. a) Cells stained with antibodies targeting MYH1 which were coupled to mCherry. b) Cells stained with antibodies targeting MYOD1 which were coupled to mCherry. Percentages indicate proportion of cells positive for the respective protein. The cells were differentiated over the course of 6 days and then fixated. Data was acquired using a FACS Symphony A1 and the mCherry channel. X-axis is measured levels of each protein as indicated in the images. Y-axis is percentage of total counts of cells. Due to a lack of sample, iX-intron with reduced seeding density was used in this comparison. The data was normalized through FlowJo to total counts of cells for each cell line. MYH1 = Myosin heavy chain 1, MYOD1 = Myogenic differentiation 1.

To measure the expression levels of muscle and pluripotency markers a Reverse Transcription Quantitative Polymerase Chain Reaction (RT-qPCR) was conducted. *MYOD1* and *POU5F1* expression were investigated as well as the downstream marker *DES*. The first two were chosen because the inserts are targeting them, both are also critical for the differentiation into skeletal myocytes. *DES* was investigated because it is a structural protein expressed in differentiated cells, it will give an indication as to how far the cells have gone in their differentiation.

iX had a *MYOD1* expression 111% that of *TBP* and iX-intron had almost double that amount at 218% *MYOD1* of *TBP* (fig. 3.12). *POU5F1* expression is reduced in both cell lines, iX-intron to 18% and iX to 4.4% of the *HBEGF* control. The *MYOD1* expression difference is multiplied when the gene expression for *DES* is investigated. iX-intron had a 1450% of *TBP* expression of *DES* which is 76 times higher than iX's expression of 19%. No expression of *MYOD1* and *DES* was found in the *HBEGF* control.

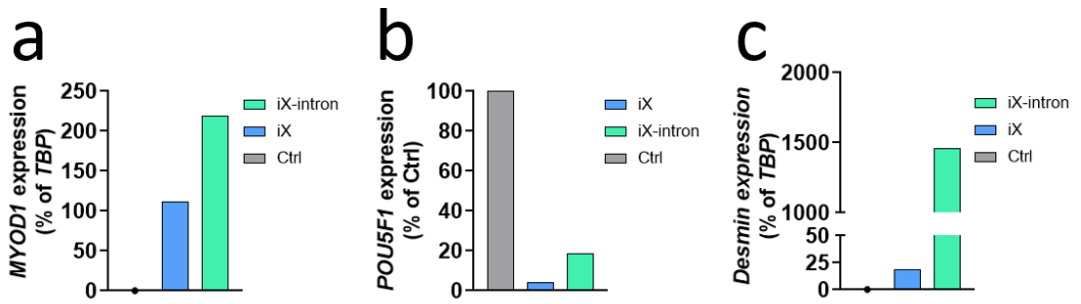

Figure 3.12: Three graphs of gene expression for **a**) *MYOD1* **b**) *POU5F1* **c**) *Desmin* with iX (blue), iX-intron (teal) and the *HBEGF* control (grey). *MYOD1* and *Desmin* are normalized to *TBP* and *POU5F1* is normalized to the *HBEGF* control. Ctrl = *HBEGF* control. *MYOD1* = Myogenic differentiation 1, *POU5F1* = Octamer binding transcription factor 4, *TBP* = TATA-box binding protein. n=1-2, where n=2 the average was used. No statistical analysis was performed due to lack of replicates.

3.2.4 Seeding Density's effect on differentiation efficiency of generated cell lines

Since the growth rate of doxycycline induced iX and iX-intron was determined to be different (fig. 3.4), a differentiation with varying seeding density was conducted to determine what effect this had on the final phenotype of the cells. The seeding density is displayed in table 2.1 of the methods. Each seeding density in this section is represented as fractions of the original density of iX and iX-intron.

Phase imaging over the course of the differentiation showed cells behaving differently depending on the seeding density (fig. 3.13). On day five, the 3/4 fraction has formed clusters whereas the 1/4 has not formed any clusters. 2/4 has less clusters than 3/4 but they are still present.

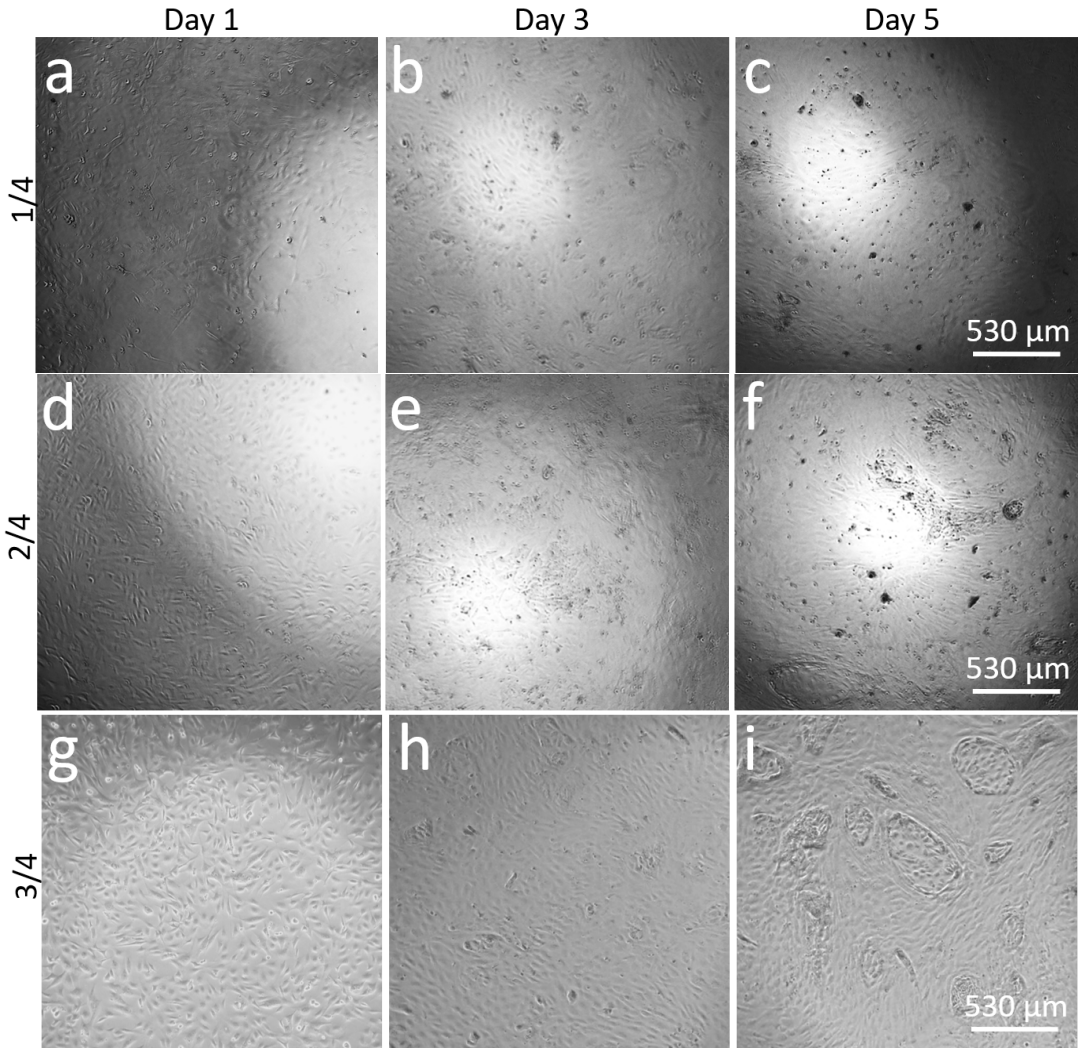

Figure 3.13: Phase images of iX-intron in differentiation media seeded on 96 well plates. The first row, a, b, c, depicts a seeding density of 1/4. The second row, d, e, f, depicts a seeding density of 2/4. The third row, g, h, i, depicts a seeding density of 3/4. Time increases from left to right, the first column is day 1, the second column is day 3, and the third column is day 5. The white bar in c indicates 530 μm. Images were acquired using the phase lens of an Invitrogen EVOS FL Digital Inverted Fluorescence Microscope.

All fractions of iX-intron seeding resulted in higher than 99% mNeonGreen positive cells (FACS figure found in Appendix A. However, there were varying levels of MYOD1 and MYH1 positive cells between the fractions (fig. 3.14). iX intron 3/4 had 52.5% positive cells, 2/4 only 41.9% and 1/4 at the highest with 67.7% of cells positive for MYH1. A similar pattern was observed for MYOD1 where the positive cells numbered 59.8%, 30.2% and 59.8% for 3/4, 2/4 and 1/4 respectively.

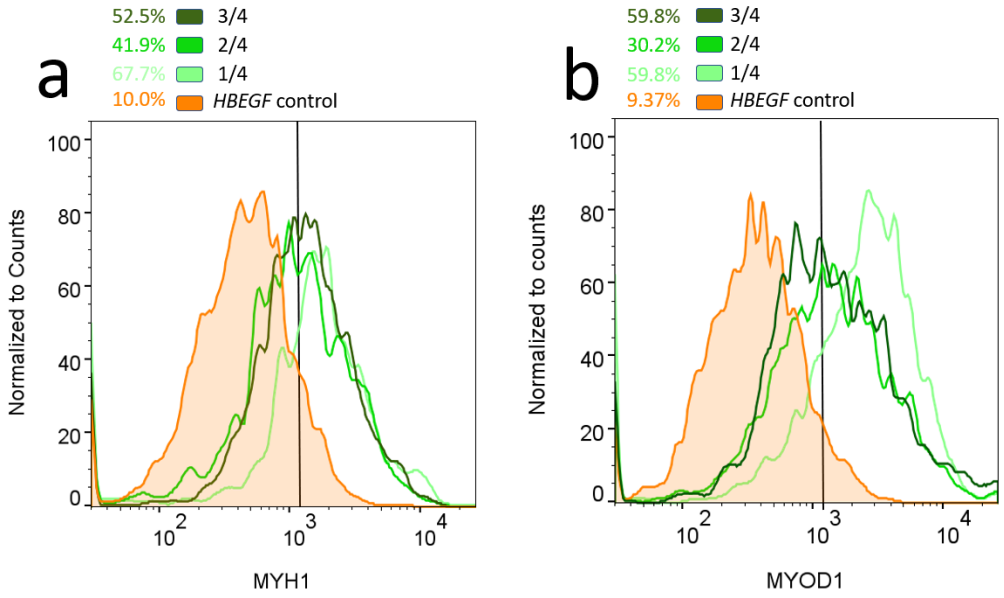

Figure 3.14: FACS results analyzed in FlowJo. iX-intron shown in green. *HBEGF* control in orange. a) Cells stained with antibodies targeting MYH1 which were coupled to mCherry. b) Cells stained with antibodies targeting MYOD1 which were coupled to mCherry. Different seeding densities of iX-intron is shown as fraction of the first differentiations seeding of 35 000 cells per 96 well. Percentages indicate proportion of cells positive for the respective protein. The cells were differentiated over the course of 6 days and then fixated. Data was acquired using a FACS Symphony A1 and the mCherry channel. X-axis is measured levels of each protein as indicated in the images. Y-axis is percentage of total counts of cells. The data was normalized through FlowJo to total counts of cells for each cell line. MYH1 = Myosin heavy chain 1, MYOD1, Myogenic differentiation 1.

The gene expression of *MYOD1*, *POU5F1* and *DES* varied depending on seeding density (fig. 3.15). The fraction with the lowest expression of *MYOD1* was 1/4 at 17% of *TBP*. The second to highest level of expression was 3/4 at 204% of *TBP* and the highest expression of *MYOD1* was 2/4 at 442% of *TBP*. Expression of *POU5F1* decreases with seeding density, the demonstrated gene levels were 18%, 11% and 9% for 3/4, 2/4 and 1/4. Lastly, *DES* expression was ten fold higher in 1/4 compared to 3/4, 19969% and 1457% respectively. The 2/4 fraction of iX-intron had the highest expression of *DES* at 30626% of *TBP*.

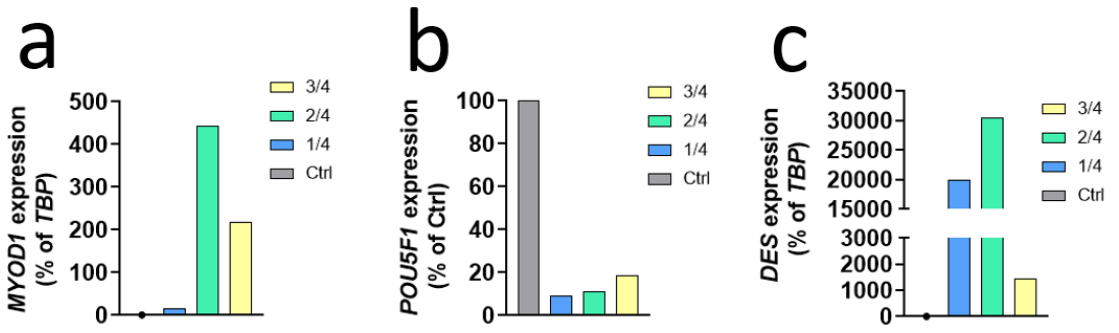

Figure 3.15: Three graphs of gene expression for different seeding densities of iX-intron, 3/4 (Yellow), 2/4 (Teal) 1/4 (blue). The genes are **a**) *MYOD1* **b**) *POU5F1* **c**) *DES*. *MYOD1* and *DES* are normalized to *TBP* and *POU5F1* is normalized to the *HBEGF* control. Ctrl = *HBEGF* control. *MYOD1* = Myogenic differentiation 1, *POU5F1* = Octamer binding transcription factor 4, *TBP* = TATA-box binding protein, n=1, no statistical testing was performed due to lack of replicates.

3.3 Differentiation of Commmercial Skeletal Myocytes

To establish a comparison for iX and iX-intron a skeletal myocyte kit was acquired from BitBio. The differentiation of the BitBio cells was tracked over the course of three days (fig. 3.16). In on day 1 the morphology of the cells was similar to that of WT hiPSCs, on day 3 the morphology had changed into that of elongated fibers.

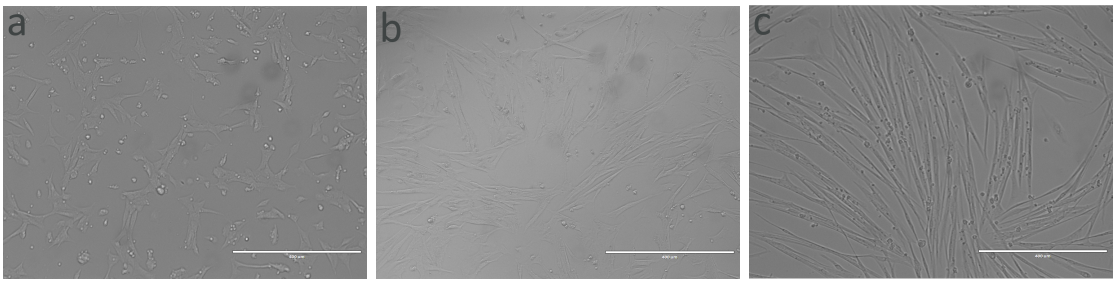

Figure 3.16: BitBio cell growth over the span of 3 days, figure 3.16 **a** was acquired 24 hours after cell seeding, **b** was acquired 48 hours after seeding and **c** shows cells 72 hours after seeding. The white bar in a, b and c indicates 400 um.

To investigate gene expression and confirm that the genes of interest where expressed a RT-qPCR was conducted. Several different probes were used, among them probes for *DES*, *MYOD1* and *POU5F1*. In figure 3.17 each of these is shown, *DES* expression has increased to 18 000% of *TBP*, *MYOD1* has increased to 305% of *TBP* and *POU5F1* has decreased to 25% of the *HBEGF* control cell line.

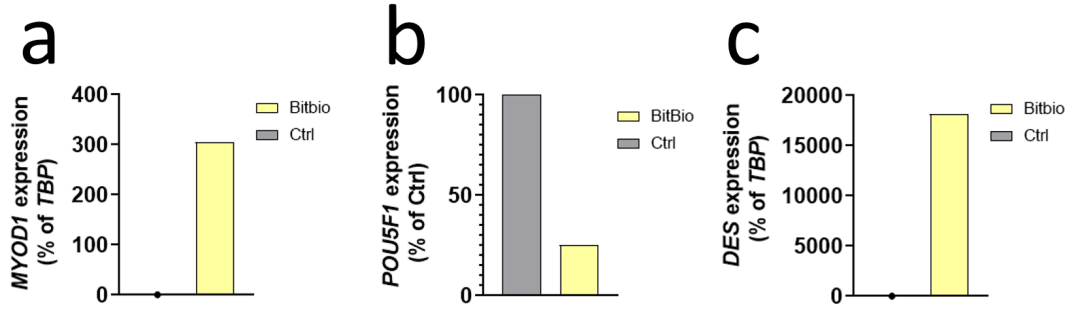

Figure 3.17: Three graphs of gene expression for *DES*, *MYOD1* and *POU5F1*. **a**) displays the gene expression of *DES* in BitBio cells and the *HBEGF* control (ctrl) cells, normalized as a percentage of the housekeeper gene *TBP*. **b**) displays the gene expression of *MYOD1* in BitBio cells and the *HBEGF* control cells, normalized as a percentage of the housekeeper gene *TBP*. **c**) displays the gene expression of *POU5F1* in BitBio cells and the *HBEGF* control cells, normalized as a percentage of the *HBEGF* control. *MYOD1* = Myogenic differentiation 1, *POU5F1* = Octamer binding transcription factor 4, *DES* = *Desmin*, *TBP* = TATA-box binding protein

Immunofluorescence imaging was performed to validate the elongated structure and to see the dispersion and homogeneity of MYOD1, OCT4 and DES. MYOD1 was

found present in most nuclei that could be discerned in the imaging, OCT4 was present in several cells but not all (fig. 3.18).

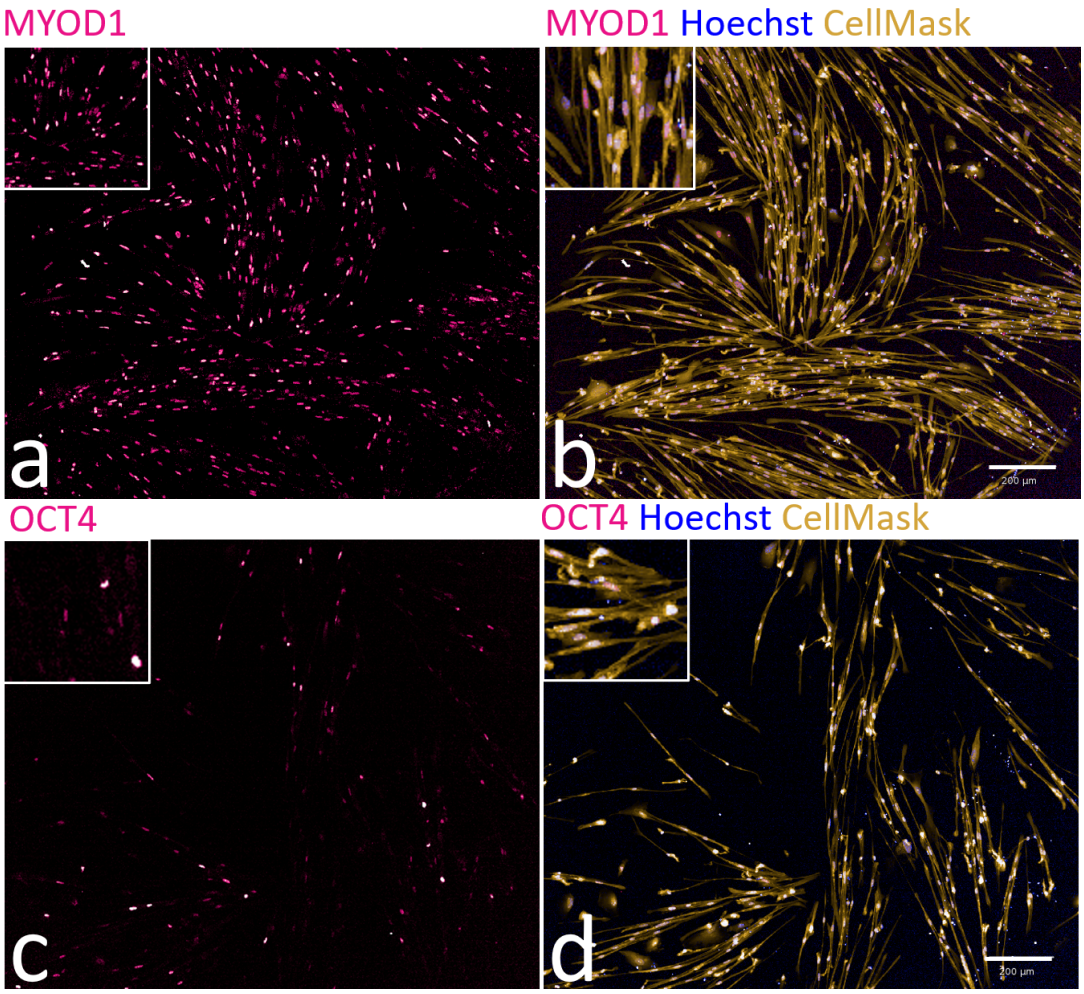

Figure 3.18: Differentiated BitBio cells, Hoechst (blue), CellMask (Yellow), MYOD1 (Pink) and OCT4 (PINK) as indicated in the images. CellMask = HCS CellMask-Deep Red, OCT4 = Octamer-binding transcription factor 4. MYOD1 = Myogenic differentation 1 , mNG = mNeonGreen Cells were fixated on the sixth day of differentiation. Images were captured with a YOKOGAWA 7000, uploaded and analyzed in Columbus.

DES was found in the cytoplasm of the cells and aligned with the CellMask, however there were still cells that did not express DES (fig. 3.19).

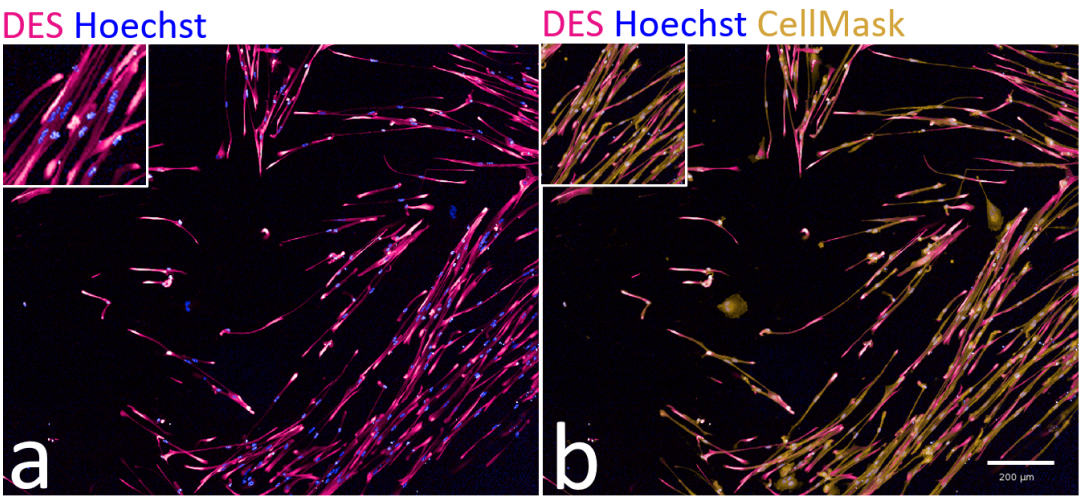

Figure 3.19: Differentiated BitBio cells stained for hoechst (blue), CellMask (Yellow) and DES (Pink), shown as indicated indicated in the images. CellMask = HCS CellMask-Deep Red, DES = Desmin. Cells were fixated on the sixth day of differentiation. Images were captured with a YOKOGAWA 7000, uploaded and analyzed in Columbus.

4

Discussion

The thesis aimed to investigate if the previously observed heterogeneity of iPSC differentiation into skeletal myocytes could be solved through modifying the expression of *MYOD1* and *POU5F1*. These two genes as well as the downstream proteins DES and MYH1 and their related genes were used to evaluate the differentiated cells.

The intron sequence modifies the expression of *MYOD1* and the shRNA targeting *POU5F1*. This affects differentiation results which is also influenced by the seeding densities of the cells. Although the in house developed cell lines express muscle markers, their morphology does not match that of the BitBio commercial skeletal myocyte kit.

4.1 Effect of intron sequence on expression levels of muscle markers

As indicated by the IF imaging, there is still room for improvement in the differentiation method to achieve a similar morphology to BitBio cells. iX and iX-intron both display a changed morphology compared to WT cells however neither show a morphology close to BitBio cells. iX and iX-intron are not elongated to the same extent as the BitBio cells, there is also no observed fusing of nuclei which is a common indication of mature skeletal myocytes [18].

The RT-qPCR shows that iX had an increased expression of *MYOD1* and the down stream marker *DES* compared to the *HBEGF* control. iX-intron has a more pronounced expression of both, which is in line with previous studies, the HBB ISV2 intron sequence increased expression levels of the transgene [38]. At the same seeding density, *MYOD1* expression measured by RT-qPCR for iX-intron was 2-fold that of iX. The difference between *DES* expression in iX and iX-intron is a testament to how much the fourfold increase in *MYOD1* affects down stream markers for myogenesis. The intron sequence was useful to increase gene expression which is reflected in the more homogeneous spread of proteins observed in the IF images.

Through flow cytometry it was confirmed that both cell lines express enough mNeonGreen to be shifted past the WT gating, the transgene was expressed in more than 99% of the cell population which the flow cytometry was performed on. However, the MYOD1 staining did not show the same trend. This could be due to the staining not working properly, the antibody had not been tested previously to running the

experiment. Acquiring a positive control for MYOD1 staining, that were not cells which went through the same differentiation protocol, would require primary cell tissue or a cell population known to contain MYOD1 in 100% of the cells which were not available. This gives the flow cytometry with MYOD1 and MYH1 a level of uncertainty as only a negative control was present for the experiments. Overall, even if iX visually performs better in the phase imaging, iX-intron expresses *MYOD1* and *DES* better and this indicates that the cell line is expressing skeletal myocytes markers more than iX at the time point of the experiments. All of this suggests that there is more at play than successful expression of transgene for differentiation.

4.2 Seeding density's effect on differentiation

As shown by IF imaging, qPCR and flow cytometry, seeding densities of doxycycline inducible iPSCs affect the differentiation efficiency. *DES* expression varies between 1400% to 31000% of *TBP*, *MYOD1* expression follows a similar pattern where expression varies between 20% to 442% of *TBP* depending on the seeding density. This indicates that cells communicate and support each other through changes in morphology and phenotype, and that a too high or too low seeding density leads to variability in the final differentiation outcome. A reason for this might be that cells which are allowed to grow past a monolayer won't be induced by the doxycycline properly and thus continue to have high levels of OCT4 present. This would halt the differentiation of the affected cells and likely halt the differentiation of adjacent cells. Seeding density will also play a role in contact inhibition and cell health, if one cell dies the cells in contact with the dying one is more likely to die as well.
In a previous study using Adeno-Associated Virus Integration Site 1 (*AAVS1*) as the target for gene editing, the seeding density's effect on differentiation outcome was not explored [3]. Among all of the seeding densities that were tried, 2/4 was the most efficient at expressing *MYOD1* and *DES*, future protocols should take this into account and also check for growth rate prior to calculating the seeding density for a differentiation. Overall clustering was reduced in tandem with the seeding density as no clusters were observed in 1/4, some in 2/4 and frequent clusters in 3/4.

4.3 Commercial skeletal myocyte comparison

The differentiated BitBio cells have an elongated structure with some appearing multinucleated. IF imaging confirms the presence of both DES and MYOD1 in the cells, the cell mask staining highlights the structure of the cells to be that of a striated nature.

Regarding expression levels, iX-intron at 2/4 and 1/4 the original seeding density are closest in comparison. Although iX-intron at 1/4 the original seeding density expresses *MYOD1* at 20% of *TBP* it still matches BitBio cells for the downstream marker *DES*. This was shown by qPCR where both cell lines expressed*DES* in between 18000% and 20000% of *TBP*. This suggests that within each cell line, the right seeding density has a larger effect than the amount of *MYOD1* for successful

expression of *DES*. However, 2/4 had higher *MYOD1* than 1/4 and than BitBio cells which also resulted in a higher level of *DES*.

The effect of the levels of *MYOD1* on downstream markers needs to be explored further as the first RT-qPCR suggested increased *MYOD1* leads to an increase in *DES* however the BitBio and Seeding density results reveal that there is more than meets the eye.
The reasons why BitBio's morphology is more mature than iX and iX-intron could be manifold, however a possible reason might be that BitBio selects single clones to grow up, this ensures that gene expression between cells will have less variance. Future attempts at differentiation should incorporate single clone selection and explore how that might affect the homogeneity.

4.4 Future experiments

To further investigate how the seeding density affects differentiation patterns and homogeneity, conducting more experiments with a larger range of seeding densities for both iX and iX-intron would be useful. Expanding the incubation period in the maintenance media could lead to better differentiation results as well. Modifying the transgenes to contain different amounts of unique shRNA targeting *POU5F1* could lead to better result. BitBio cells still express some *POU5F1* compared to the *HBEGF* control, this indicates a complete silencing of *POU5F1* might not be necessary. Transfecting iPSCs again with the plasmids and selecting single clones to grow up cultures could result in higher levels of homogeneity, expanding this to different original iPSC cell lines would solidify the results.

4.5 Implications

Integrating the transgenes required for differentiation next to *HBEGF* allows for further modifications to enable transgenes to be introduced at *AAVS1*. The opportunity to change phenotype of iPSCs without affecting the *AAVS1* is of importance because *AAVS1* is sometimes considered a safe harbour for genome engineering [40]. Testing cell type specific treatments targeting AVVS1 would be possible using the protocol developed in this thesis.

Reliable differentiation of skeletal myocytes from hiPSCs provide a new platform to investigate genetic variants of disease in skeletal myocytes. There is already robust methods to edit hiPSCs, being able to efficiently change these hiPSCs into skeletal myocytes or any other tissue specific cell type would allow for shorter time frames for new modalities. An established protocol to differentiate stem cells into a phenotype using the Xential method could act as a proof of concept for applying it to other cell varieties and open up new possibilities for fast acquirement of relevant cell types.

4.6 Conclusion

The aim of the thesis has been to address the observed heterogeneity of hiPSC differentiation into skeletal myocytes by modifying the gene expression of *MYOD1* and *POU5F1*. In conjunction, seeding density's effect on differentiation outcomes was also explored. The HBB IVS2 intron sequence had a significant impact on the expression of muscle markers and homogeneity, indicating its utility in enhancing or modifying differentiation efficiency.

Challenges still remain despite the enhanced ability by the intron sequence. Developed cell lines did not achieve morphology akin to commercially available skeletal myocytes. Seeding density was determined to be a crucial factor to optimize differentiation efficiency and achieving consistent outcomes.

Establishing protocols using the Xential method breaks new ground for fast acquisition of relevant cell types. Expression levels and seeding density are key to the establishment of such protocols and successful incorporation of these could accelerate disease modelling and regenerative medicine.

Bibliography

[1] T. Akiyama, S. Sato, N. Chikazawa-Nohtomi, A. Soma, H. Kimura, S. Wakabayashi, S. Ko, and M. Ko, "Efficient differentiation of human pluripotent stem cells into skeletal muscle cells by combining rna-based myod1-expression and pou5f1-silencing," *Scientific Reports*, vol. 8, 01 2018.

[2] R. Abujarour, M. Bennett, B. Valamehr, M. Robinson, D. Robbins, T. Le, K. Lai, and P. Flynn, "Myogenic differentiation of muscular dystrophy-specific induced pluripotent stem cells for use in drug discovery," *Stem cells translational medicine*, vol. 3, 01 2014.

[3] M. Pawlowski, D. Ortmann, A. Bertero, J. Tavares, R. Pedersen, L. Vallier, and M. Kotter, "Inducible and deterministic forward programming of human pluripotent stem cells into neurons, skeletal myocytes, and oligodendrocytes," *Stem Cell Reports*, vol. 8, 03 2017.

[4] G. Shefer and Z. Yablonka-Reuveni, "Isolation and culture of skeletal muscle myofibers as a means to analyze satellite cells," in *Basic Cell Culture Protocols*. New Jersey: Humana Press, 2004, pp. 281–304.

[5] A. Soriano-Arroquia, P. D. Clegg, A. P. Molloy, and K. Goljanek-Whysall, "Preparation and culture of myogenic precursor cells/primary myoblasts from skeletal muscle of adult and aged humans," *J. Vis. Exp.*, no. 120, Feb. 2017.

[6] K. Suetterlin, R. Männikkö, E. Matthews, L. Greensmith, M. Hanna, H. Bostock, and S. Tan, "Excitability properties of mouse and human skeletal muscle fibres compared by muscle velocity recovery cycles," *Neuromuscular Disorders*, vol. 32, no. 4, pp. 347–357, 2022.

[7] K. Joshi, S. S. Hassan, and P. Ramaraj, "Differential biological effects of dehydroepiandrosterone (dhea) between mouse (b16f10) and human melanoma (blm) cell lines," *Dermato-Endocrinology*, vol. 9, p. e1389360, 2017.

[8] J. L. Almeida, C. R. Hill, and K. D. Cole, "Mouse cell line authentication," *Cytotechnology*, vol. 66, pp. 133–147, 2013.

[9] S. Li, N. Akrap, S. Cerboni, M. J. Porritt, S. Wimberger, A. Lundin, C. ller, M. Firth, E. Gordon, B. Lazovic, A. ska, L. S. Pane, M. A. Coelho, G. Ciotta, G. Pellegrini, M. Sini, X. Xu, S. Mitra, M. Bohlooly-Y, B. J. M. Taylor, G. Sienski, and M. Maresca, "Author Correction: Universal toxin-based selection for precise genome engineering in human cells," *Nat Commun*, vol. 12, no. 1, p. 2832, May 2021.

[10] K. Takahashi, K. Tanabe, M. Ohnuki, M. Narita, T. Ichisaka, K. Tomoda, and S. Yamanaka, "Induction of pluripotent stem cells from adult human fibroblasts by defined factors," *Cell*, vol. 131, no. 5, pp. 861–872, 2007.

[11] J. Yu, M. A. Vodyanik, K. Smuga-Otto, J. Antosiewicz-Bourget, J. L. Frane, S. Tian, J. Nie, G. A. Jonsdottir, V. Ruotti, R. Stewart, I. I. Slukvin, and J. A. Thomson, "Induced pluripotent stem cell lines derived from human somatic cells," *Science*, vol. 318, no. 5858, pp. 1917–1920, Dec. 2007.

[12] L. Tesařová, P. Šimara, S. Stejskal, and I. Koutná, "The aberrant dna methylation profile of human induced pluripotent stem cells is connected to the reprogramming process and is normalized during in vitro culture," *Plos One*, vol. 11, p. e0157974, 2016.

[13] Y. Cheng, M. Xu, G. Chen, J. Beers, C. Z. Chen, C. Liu, J. Zou, and W. Zheng, "A protocol for culture and characterization of human induced pluripotent stem cells after induction," *Current Protocols*, vol. 3, 2023.

[14] X. Fan, L. Cyganek, K. Nitschke, S. Uhlig, P. Nuhn, K. Bieback, D. Duerschmied, I. El-Battrawy, X. Zhou, and I. Akin, "Functional characterization of human induced pluripotent stem cell-derived endothelial cells," *Int. J. Mol. Sci.*, vol. 23, no. 15, p. 8507, Jul. 2022.

[15] B. Ulmer, A. Stoehr, M. L. Schulze, S. Patel, M. Guček, I. Mannhardt, S. Funcke, E. Murphy, T. Eschenhagen, and A. Hansen, "Contractile work contributes to maturation of energy metabolism in hipsc-derived cardiomyocytes," *Stem Cell Reports*, vol. 10, pp. 834–847, 2018.

[16] W. R. Frontera and J. Ochala, "Skeletal muscle: a brief review of structure and function," *Calcif. Tissue Int.*, vol. 96, no. 3, pp. 183–195, Mar. 2015.

[17] R. S. Stephenson, P. Agger, P. P. Lunkenheimer, J. Zhao, M. Smerup, P. F. Niederer, R. H. Anderson, and J. C. Jarvis, "The functional architecture of skeletal compared to cardiac musculature: myocyte orientation, lamellar unit morphology, and the helical ventricular myocardial band," *Clinical Anatomy*, vol. 29, pp. 316–332, 2015.

[18] A. Cutler, A. H. Corbett, and G. K. Pavlath, "Biochemical isolation of myonuclei from mouse skeletal muscle tissue," *Bio-Protocol*, vol. 7, 2017.

[19] A. Bareja, J. A. Holt, G. Luo, C. Chang, J. Lin, A. C. Hinken, J. M. Freudenberg, W. E. Kraus, W. J. Evans, and A. N. Billin, "Human and mouse skeletal muscle stem cells: convergent and divergent mechanisms of myogenesis," *PLoS One*, vol. 9, no. 2, p. e90398, Feb. 2014.

[20] B. C. Das and A. Tyagi, "Chapter 23 - stem cells: A trek from laboratory to clinic to industry," in *Animal Biotechnology*, A. S. Verma and A. Singh, Eds. San Diego: Academic Press, 2014, pp. 425–450.

[21] K. Takahashi and S. Yamanaka, "Induction of pluripotent stem cells from mouse embryonic and adult fibroblast cultures by defined factors," *Cell*, vol. 126, no. 4, pp. 663–676, Aug. 2006.

[22] P. Hasty, A. Bradley, J. Morris, D. Edmondson, J. Venuti, E. Olson, and W. Klein, "Muscle deficiency and neonatal death in mice with a targeted mutation in the myogenin gene," *Nature*, vol. 364, pp. 501–6, 09 1993.

[23] Y. Nabeshima, K. Hanaoka, M. Hayasaka, E. Esumi, S. Li, and I. Nonaka, "Myogenin gene disruption results in perinatal lethality because of severe muscle defect," *Nature*, vol. 364, pp. 532–5, 09 1993.

[24] F. Iberite, E. Gruppioni, and L. Ricotti, "Skeletal muscle differentiation of human iPSCs meets bioengineering strategies: perspectives and challenges," *NPJ Regen. Med.*, vol. 7, no. 1, p. 23, Apr. 2022.

[25] T. Sato, "Induction of skeletal muscle progenitors and stem cells from human induced pluripotent stem cells," *J. Neuromuscul. Dis.*, vol. 7, no. 4, pp. 395–405, 2020.

[26] R. Abujarour, M. Bennett, B. Valamehr, T. T. Lee, M. Robinson, D. Robbins, T. Le, K. Lai, and P. Flynn, "Myogenic differentiation of muscular dystrophy-specific induced pluripotent stem cells for use in drug discovery," *Stem Cells Transl. Med.*, vol. 3, no. 2, pp. 149–160, Feb. 2014.

[27] J. Chal, M. Oginuma, Z. Al Tanoury, B. Gobert, O. Sumara, A. Hick, F. Bousson, Y. Zidouni, C. Mursch, P. Moncuquet, O. Tassy, S. Vincent, A. Miyanari, A. Bera, J.-M. Garnier, G. Guevara, M. Hestin, L. Kennedy, S. Hayashi, B. Drayton, T. Cherrier, B. Gayraud-Morel, E. Gussoni, F. Relaix, S. Tajbakhsh, and O. Pourquié, "Differentiation of pluripotent stem cells to muscle fiber to model duchenne muscular dystrophy," *Nat. Biotechnol.*, vol. 33, no. 9, pp. 962–969, Sep. 2015.

[28] S. Albini, P. Coutinho, B. Malecova, L. Giordani, A. Savchenko, S. V. Forcales, and P. L. Puri, "Epigenetic reprogramming of human embryonic stem cells into skeletal muscle cells and generation of contractile myospheres," *Cell Rep.*, vol. 3, no. 3, pp. 661–670, Mar. 2013.

[29] Y. Xu and Z. Li, "CRISPR-Cas systems: Overview, innovations and applications in human disease research and gene therapy," *Comput. Struct. Biotechnol. J.*, vol. 18, pp. 2401–2415, Sep. 2020.

[30] X. Yao, X. Wang, X. Hu, Z. Liu, J. Liu, H. Zhou, X. Shen, Y. Wei, Z. Huang, W. Ying, Y. Wang, Y.-H. Nie, C.-C. Zhang, S. Li, L. Cheng, Q. Wang, Y. Wu, P. Huang, Q. Sun, L. Shi, and H. Yang, "Homology-mediated end joining-based targeted integration using CRISPR/Cas9," *Cell Res.*, vol. 27, no. 6, pp. 801–814, Jun. 2017.

[31] M. Asmamaw and B. Zawdie, "Mechanism and applications of CRISPR/Cas-9-mediated genome editing," *Biologics*, vol. 15, pp. 353–361, Aug. 2021.

[32] B.-C. Geng, K.-H. Choi, S.-Z. Wang, P. Chen, X.-D. Pan, N.-G. Dong, J.-K. Ko, and H. Zhu, "A simple, quick, and efficient CRISPR/Cas9 genome editing method for human induced pluripotent stem cells," *Acta Pharmacol. Sin.*, vol. 41, no. 11, pp. 1427–1432, Nov. 2020.

[33] A. T. Das, L. Tenenbaum, and B. Berkhout, "Tet-on systems for doxycycline-inducible gene expression," *Curr. Gene Ther.*, vol. 16, no. 3, pp. 156–167, Jun. 2016.

[34] C. Fellmann, T. Hoffmann, V. Sridhar, B. Hopfgartner, M. Muhar, M. Roth, D. Y. Lai, I. A. M. Barbosa, J. S. Kwon, Y. Guan, N. Sinha, and J. Zuber, "An optimized microRNA backbone for effective single-copy RNAi," *Cell Rep.*, vol. 5, no. 6, pp. 1704–1713, Dec. 2013.

[35] X.-Y. Wang, Q.-J. Du, W.-L. Zhang, D.-H. Xu, X. Zhang, Y.-L. Jia, and T.-Y. Wang, "Enhanced transgene expression by optimization of poly a in transfected CHO cells," *Front. Bioeng. Biotechnol.*, vol. 10, p. 722722, Jan. 2022.

[36] R. E. Sizer and R. J. White, "Use of ubiquitous chromatin opening elements (UCOE) as tools to maintain transgene expression in biotechnology," *Comput. Struct. Biotechnol. J.*, vol. 21, pp. 275–283, 2023.

[37] L. Hostettler, L. Grundy, S. Käser-Pébernard, C. Wicky, W. R. Schafer, and D. A. Glauser, "The bright fluorescent protein mNeonGreen facilitates protein expression analysis*in vivo*," *G3 (Bethesda)*, vol. 7, no. 2, pp. 607–615, Feb. 2017.

[38] A. R. Buchman and P. Berg, "Comparison of intron-dependent and intron-independent gene expression," *Mol. Cell. Biol.*, vol. 8, no. 10, pp. 4395–4405, Oct. 1988.

[39] M. Kimura, A. Takatsuki, and I. Yamaguchi, "Blasticidin S deaminase gene from aspergillus terreus (BSD): a new drug resistance gene for transfection of mammalian cells," *Biochim. Biophys. Acta Gene Struct. Expression*, vol. 1219, no. 3, pp. 653–659, Nov. 1994.

[40] H. Hayashi, Y. Kubo, M. Izumida, and T. Matsuyama, "Efficient viral delivery of cas9 into human safe harbor," *Sci. Rep.*, vol. 10, no. 1, p. 21474, Dec. 2020.

A

Appendix 1

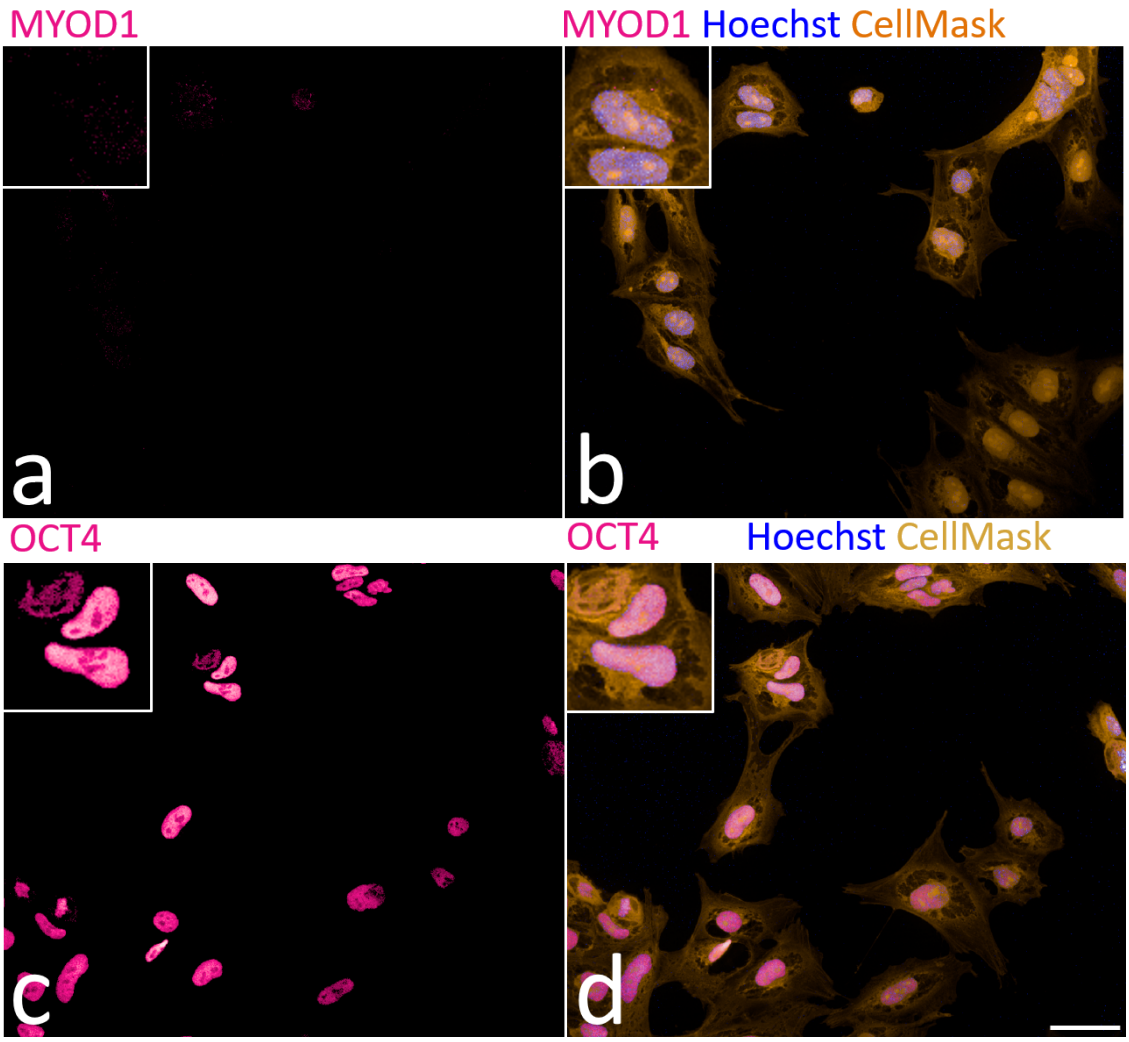

Figure A.1: Wild-type iPSCs with each staining shown as indicated in the image. **a** MYOD1, **b** MYOD1, Hoechst, CellMask, **c** OCT4, **d** OCT4, Hoechst, CellMask, CellMask = HCS CellMask-Deep Red, MYOD1 = Myogenic Differentiation 1, OCT4 = Octamer-binding transcription factor 4, WT=wild-type. Images were captured with a YOKOGAWA 7000, uploaded and analyzed in Columbus.

Desmin was not found in the wild-type iPSCs as shown in figure A.2 **a** and **b**, the first image displays Hoechst staining in blue and there is no pink Desmin in the image to be observed. A.2 **b** confirms there is a cell structure a part from the nuclei stained by hoechst, and still no Desmin was observed.

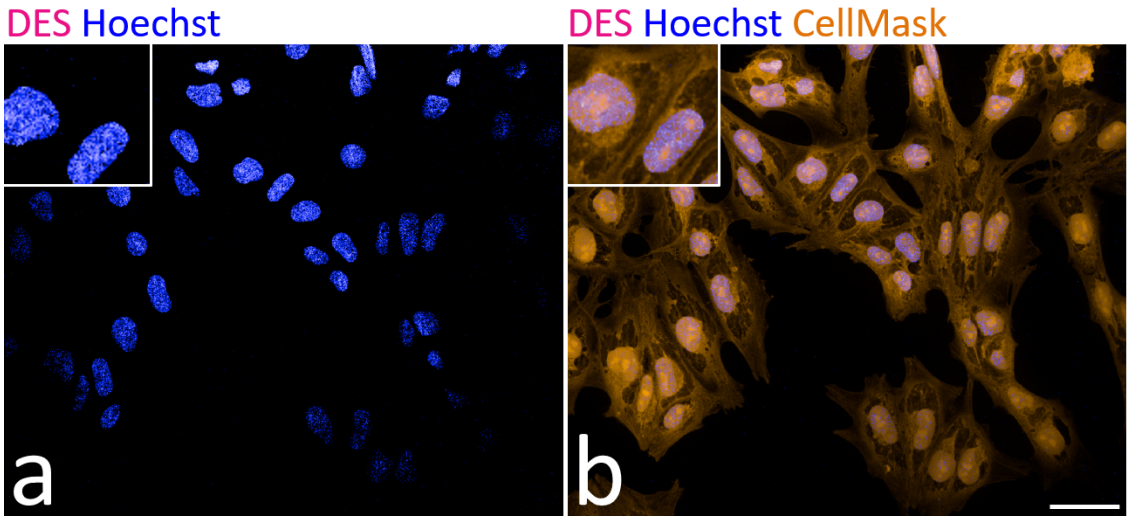

Figure A.2: **a**, Immunofluorescence stained WT iPSC cells for Hoechst (blue), DES (Pink) and HCS CellMask-Deep Red (Yellow) only the filter for DES and Hoechst turned on. **b**, The image in **a** with all filters turned on. DES = Desmin CellMask = HCS CellMask-Deep Red, WT=wild-type. Images were captured with a YOKOGAWA 7000, uploaded and analyzed in Columbus.

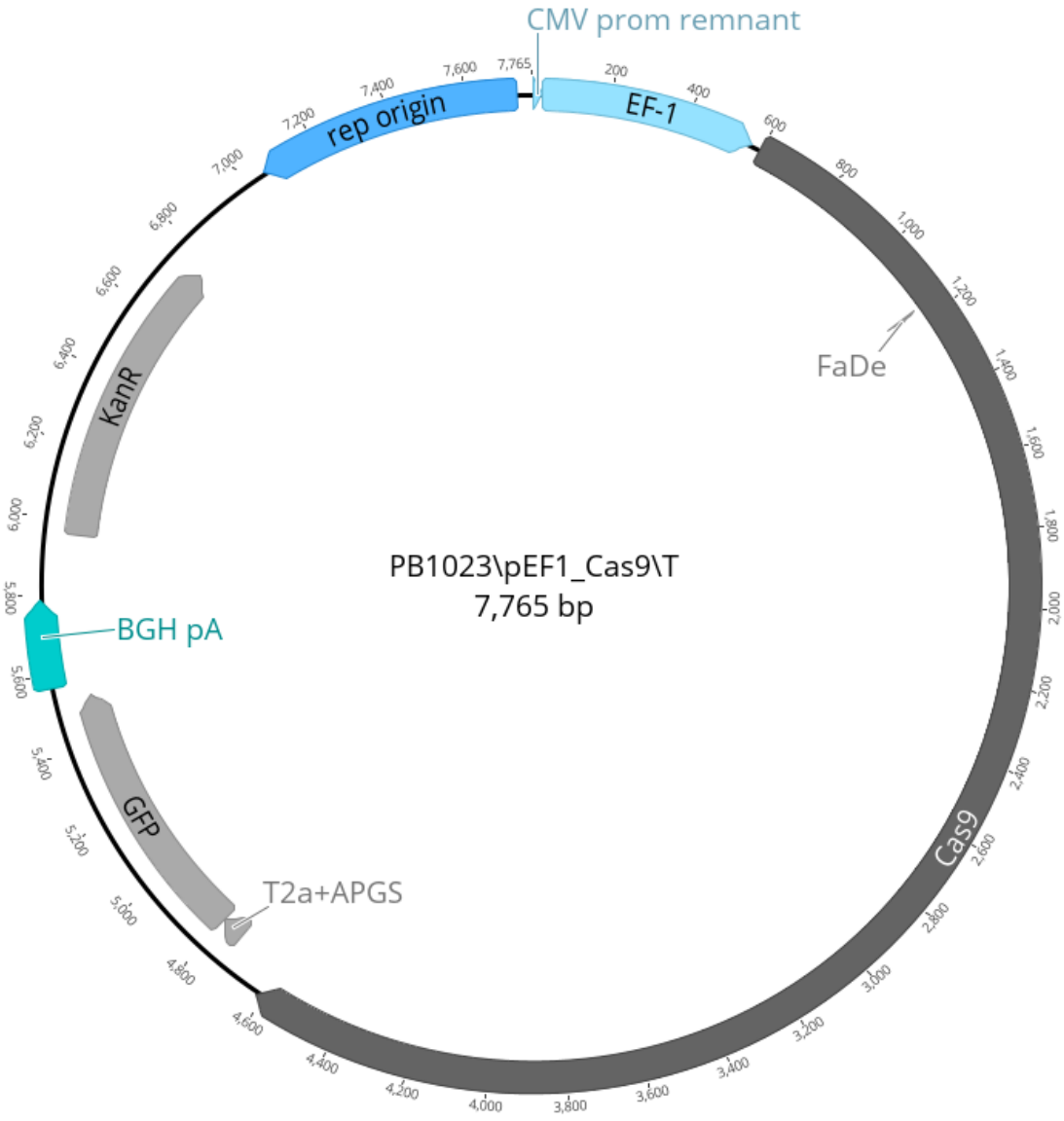

Figure A.3: Plasmid map of SpCas9. Contains Kanamycin resistance, origin of replication, CMV promoter remnant, Elongation factor 1, SpCas9, GFP and lastly the polyadenylation tail. GFP = green Fluorescent protein.

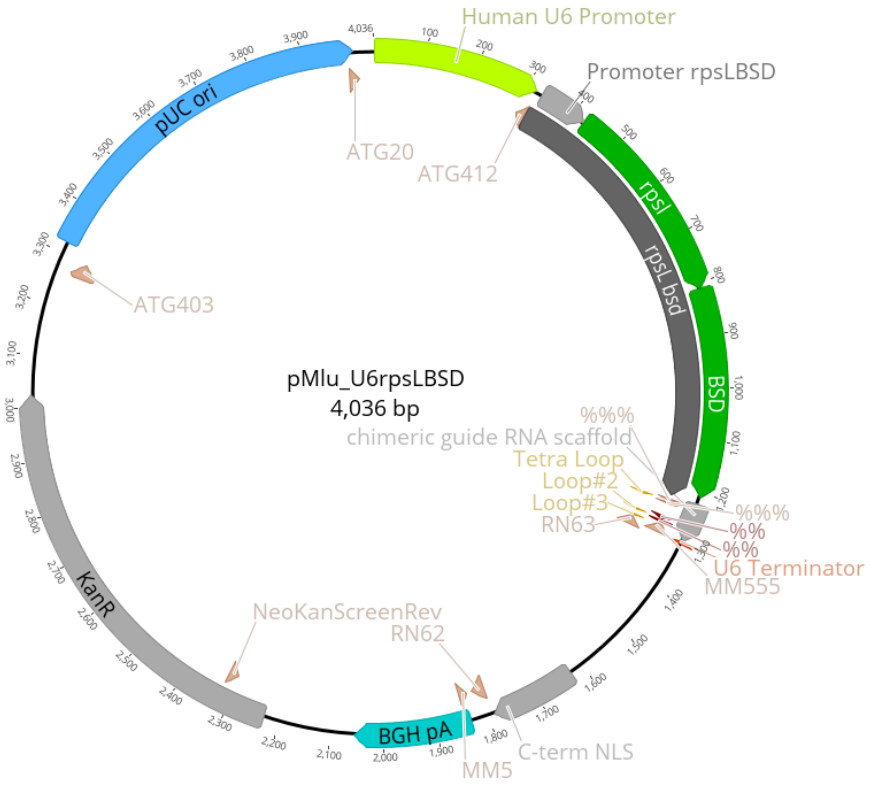

Figure A.4: Bacterial Plasmid map of sgRNA. pUC ori = Origin of replication, followed by a U6 promoter. Blasticidin (BSD) resistance and Stroptomycin resistance (rpsl) followed by the RNA scaffold and a U6 terminators. To target the thrid exon of *HBEGF* the protospacer sequence should be added right before the scaffold and it should be GGGTGATGTTGCCTGACCGG. Following the transcriptional unit, the C-terminus is located with an NLS tag to bring it to the nucleus. Then there is the polyadenylation tail followed by Kanamycin reistance.

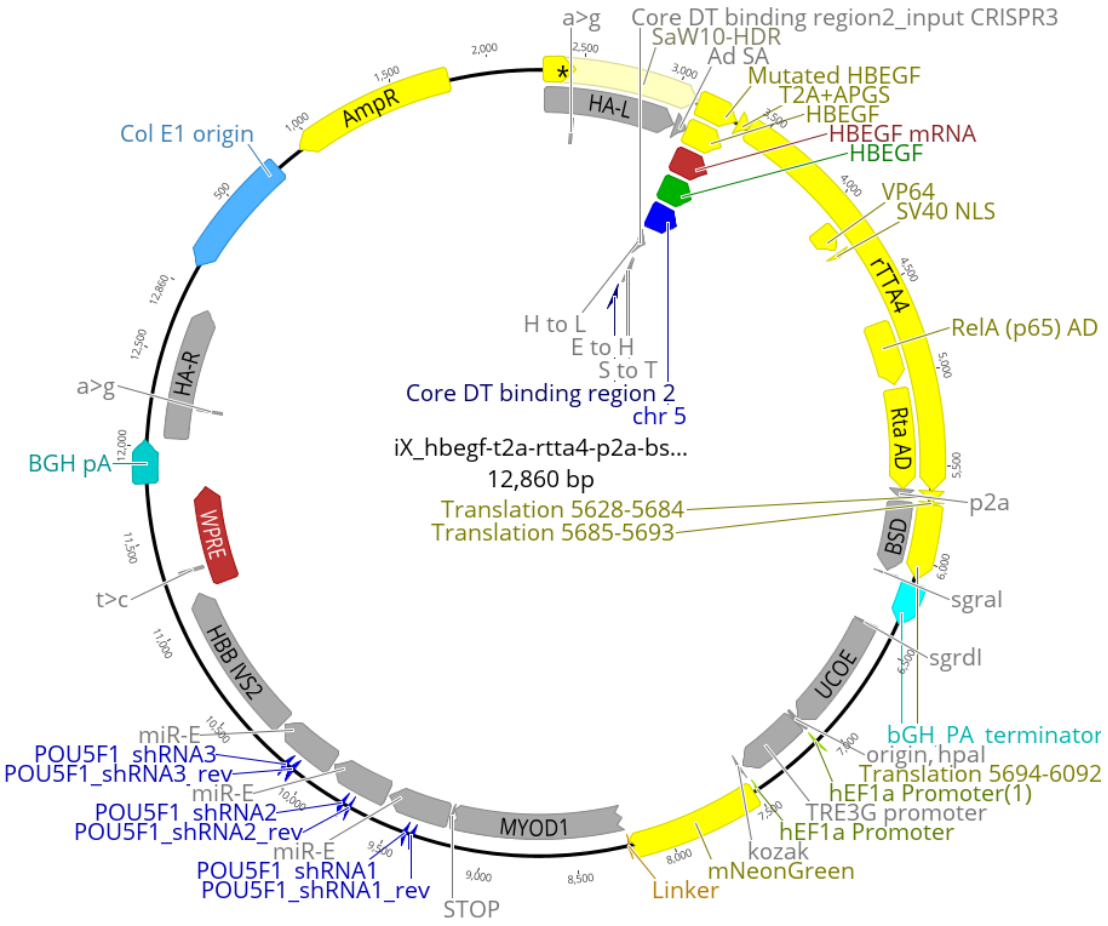

Figure A.5: Full bacterial plasmid map of iX as described in methods 2.2, with the addition a left and right homology arm, an origin of replication and Ampicilin resistance (AmpR).

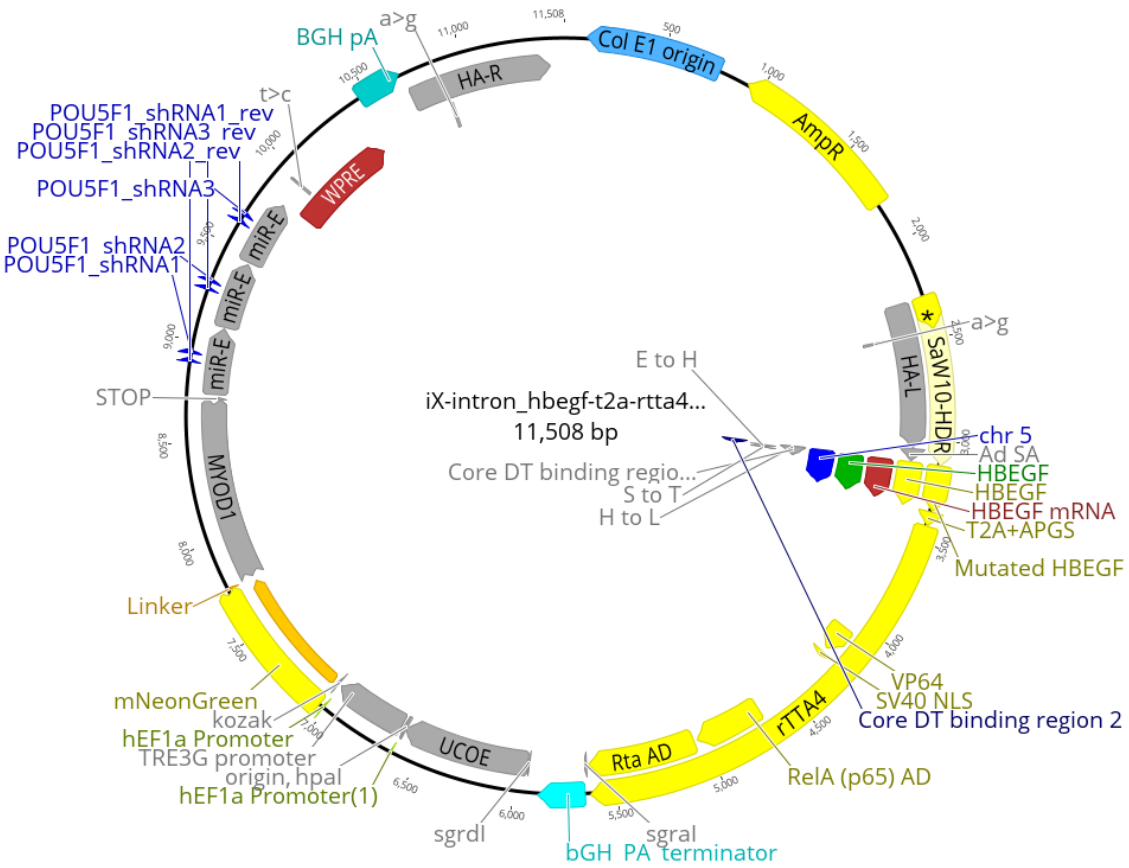

Figure A.6: Full bacterial plasmid map of iX-intron as described in methods 2.2, with the addition a left and right homology arm, an origin of replication and Ampicilin resistance (AmpR).

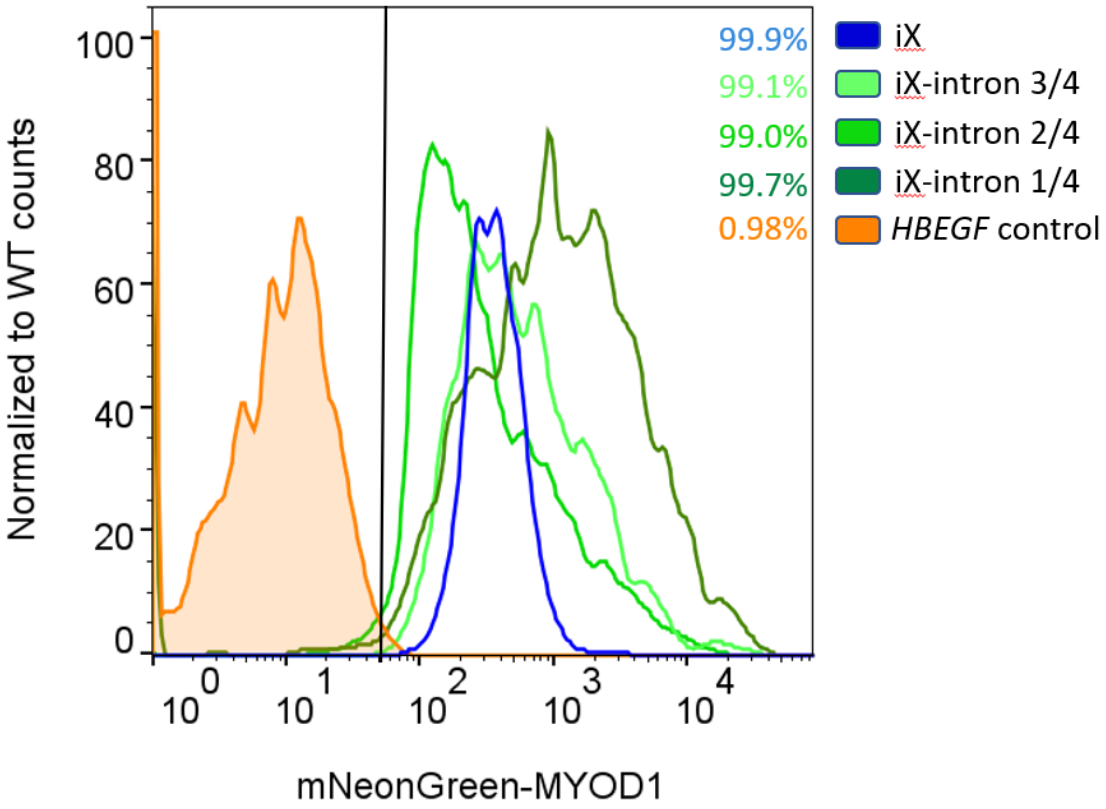

Figure A.7: FACS results analyzed in FlowJo. iX shown in blue, iX-intron shown in shades of green based on fractions. Percentages indicate proportion of cells positive for mNeonGreen coupled to MYOD1. The cells were differentiated over the course of 6 days and then fixated. Data was acquired using a FACS Symphony A1 and the mCherry channel. X-axis is measured levels of mNeonGreen coupled to MYOD1 through the AlexaFluor 488 channel. Y-axis is percentage of total counts of cells. The data was normalized through FlowJo to total counts of cells for each cell line. MYOD1 = Myogenic Differentiation 1.

DEPARTMENT OF LIFE SCIENCE
CHALMERS UNIVERSITY OF TECHNOLOGY
Gothenburg, Sweden
www.chalmers.se

CHALMERS
UNIVERSITY OF TECHNOLOGY